A&A 443, 61–78 (2005)
DOI: 10.1051/0004-6361:20040422

Astronomy & Astrophysics

An optical imaging study of $0.4 \leq z \leq 0.8$ quasar host galaxies⋆,⋆⋆

II. Analysis and interpretation

E. Örndahl[1,2] and J. Rönnback[2]

[1] Tuorla Observatory, Väisäläntie 20, 215 00 Piikkiö, Finland
e-mail: eva.orndahl@utu.fi
[2] Department of Astronomy and Space Physics, Uppsala University, Box 515, 751 20 Uppsala, Sweden

Received 10 March 2004 / Accepted 22 June 2005

ABSTRACT

We performed optical imaging of 102 radio-loud and radio-quiet quasars at $z = 0.4-0.8$, of which 91 fields were found suitable for host galaxy analysis after the deselection of saturated and otherwise flawed images. The data sets were obtained mainly in the R band, but also in the V and I or Gunn i band, and were presented in Rönnback et al. (1996, MNRAS, 283, 282) and Örndahl et al. (2003, A&A, 404, 883). In this paper we combine the two above-mentioned samples and also separately discuss additional hosts, extracted from data taken by Wold et al. (2000, MNRAS, 316, 267; 2001, MNRAS, 323, 231). The joint sample forms a sizeable fraction of the to-date total number of observed sources at intermediate redshifts and increases the number of resolved radio-quiet hosts at $z > 0.4$ considerably. Equal numbers of radio-loud and radio-quiet objects were observed, resulting in a detection rate of 79% for the radio-loud hosts and 66% for the radio-quiet hosts. Profile fitting could only be carried out for a minority of the sample, but it results in predominantly elliptical morphologies. This is consistent with the mean values of the axial ratios, for which we find $b/a \gtrsim 0.8$ for both radio-quiet and radio-loud hosts, just as in the case of normal elliptical galaxies. The mean absolute magnitudes of the radio-loud and radio-quiet hosts is $M_R = -23.5$ in both cases. This similarity between the mean magnitudes of the two types of host galaxy is also seen in the other imaged bands. While the radio-loud host absolute R magnitudes are correlated with redshift, only a weak trend of the same sort is seen for the radio-quiet host magnitudes. Note, however, that the sample is not fully resolved and that the detection limit, in combination with the relationship between host and nuclear luminosity, may conspire in creating the illusion of an upturn in magnitude. The average nucleus-to-host galaxy luminosity ratios of the radio-loud and radio-quiet objects do not differ significantly in any band, nor is the difference between the average luminosity ratios of flat spectrum and steep spectrum radio-loud quasars larger than 1.5σ. Thus, no effect of beaming (as expected in the unifying scheme) is seen. The colours of both radio-loud and radio-quiet host galaxies are found to be as blue as present-day late-type spirals and starburst galaxies. These blue colours are most likely due neither to galaxy evolution over the range, which only gives rise to a colour shift of ∼0.2 mag, nor to scattered nuclear light, since colours determined from annular apertures yield very similar results. Since close companions in projection are not uncommon (and a few sources even exhibit tidal tail-like features and other signs of interaction), ongoing star formation is a reasonable explanation of the blue host colours. As multiple-band imaging primarily was carried out for quasars showing indications of the presence of a host galaxy, the colour analysis results are valid for host galaxies which are large, bright, have low nucleus-to-host luminosity ratios, and/or display large scale disturbances, but cannot however safely be generalised to hold for the quasar host galaxy population at intermediate redshift as a whole.

Key words. galaxies: active – galaxies: quasars: general – galaxies: fundamental parameters – galaxies: photometry

1. Introduction

Investigations of quasar host galaxies have mainly concentrated on objects at low redshift ($z \lesssim 0.3-0.4$) where the host properties are relatively easily determined. From ground-based, as well as Hubble Space Telescope (HST), observations at both optical and near-infrared wavelengths it has been shown that the host galaxy luminosities at low redshift correspond to a few times that of a present-day Schechter L^* galaxy (Bahcall et al. 1997; McLeod & McLeod 2001), where the hosts of radio-quiet quasars (RQQ) also seem to be fainter than those of radio-loud quasars (RLQ) by ∼0.5 mag (Boyce et al. 1998; Dunlop et al. 2003). Recent advances in telescope technology have stimulated large interest in hosts at $z \gtrsim 2$. At such redshifts

⋆ Based on observations made with the Nordic Optical Telescope operated on the island of La Palma jointly by Denmark, Finland, Iceland, Norway, and Sweden, in the Spanish Observatorio del Roque de los Muchachos of the Instituto de Astrofísica de Canarias.

⋆⋆ Appendices A and B are only available in electronic form at http://www.edpsciences.org

the challenge of resolving the host galaxies becomes greater, but in general the RLQ hosts seem to have brightened considerably more than RQQ hosts (Kukula et al. 2001; Falomo et al. 2001; Ridgway et al. 2001). By studying the intermediate redshift range, the knowledge of host galaxies at different regimes can be consolidated and important constraints be provided on the evolution of quasar hosts, as well as on the quasar phenomenon itself.

The earliest studies of intermediate redshift host galaxies were carried out in the optical (Gehren et al. 1984; Romanishin & Hintzen 1989), with results showing bright, compact hosts for which no morphology could be determined conclusively. Later investigations have been performed mainly in the near-infrared, where the contrast between host and nuclear light is greater (Carballo et al. 1998; Kotilainen et al. 1998; Kotilainen & Falomo 2000; Márquez et al. 1999, 2001), resulting in host luminosities a few factors of L^* brighter than those obtained at lower redshifts. Since RLQ:s have been targetted almost exclusively, the difference in mean magnitude between RLQ and RQQ host galaxies is not very well studied at these redshifts.

Most imaging studies have concentrated on the issues of morphology and luminosity and have been carried out using only a single photometric band, making colour information scarce even at low redshifts. The difficulties associated with host galaxy spectrum extraction would seem to make broad-band colours an interesting alternative method for obtaining clues to the composition of the host stellar populations, but in spite of this it has been little exercised. Only recently have reasonably large near-infrared-to-optical colour studies been undertaken at low redshift (Dunlop et al. 2003; Jahnke 2002; Jahnke et al. 2004). The little data existing for intermediate redshifts has mainly suggested blue colours of the host galaxies (Romanishin & Hintzen 1989; Véron-Cetty & Woltjer 1990; Kirhakos et al. 1999; Sánchez et al. 2004).

Host galaxy colours as blue as late-type galaxies were also found in Rönnback et al. (1996, hereafter R96), which forms the first part of our investigation of RLQ and RQQ in the redshift interval $0.4 \leq z \leq 0.8$. The second, main part was published in Örndahl et al. (2003, hereafter Paper I). Taken together, the two parts comprise ∼50% of the collected total number of the to-date investigated sources at intermediate redshifts, and increase the number of observed RQQ in this range significantly. The observations were carried out in the R, V, and I or Gunn i band, and broad-band colours have been obtained for part of the sample. In addition to the sources observed by us, we have also been given access to data for the intermediate redshift quasars observed by Wold et al. (2000, 2001), for which a further eight host galaxy detections were made.

The layout of this paper is as follows. In Sect. 2 the sample characteristica are detailed together with error estimation and host galaxy detection statistics, summarising the main points of R96 and Paper I. In Sect. 3 the Wold data set is presented, with images and luminosity profiles shown in Appendix A. In Sect. 4 we derive and address the morphology and axial ratios (Sect. 4.1), mean absolute magnitudes and luminosity ratios (Sect. 4.2), and the colours of both quasars and hosts (Sect. 4.3). The host colours derived in this paper are compared to those of other studies in Sect. 4.4. Section 5 summarises the results, with notes on selected objects presented in Appendix B. Throughout this paper we adopt an Einstein-de Sitter universe ($q_0 = 0.5$) and a Hubble constant of $H_0 = 75\ \mathrm{km\,s^{-1}\,Mpc^{-1}}$.

2. Observations and data analysis

The sample of 102 objects is subdivided into two parts, the first of which comprises 23 objects and was presented in R96. This data set was acquired using the ESO 3.5 m NTT in January 1994, whereas the second part of the sample (79 objects) was imaged at the Nordic Optical Telescope 2.56 m instrument in June and October 1994 and December 1998 and was described in Paper I. These two subsamples will hereafter be referred to as the NTT and the NOT sample.

2.1. Sample characteristica

The quasars of both samples were selected from the catalogues of Véron-Cetty & Véron (1993) and Hewitt & Burbidge (1993), where the selection criteria used were the redshift range and the constraints imposed by the sky coordinates at the observation site. The distribution of redshifts and quasar apparent V magnitude, as listed for the objects in the NASA/IPAC Extragalactic Database (NED), are shown in Fig. 1. All objects were imaged in the R band, and additional fields were taken in the V and/or I or Gunn i band for objects where the presence of a host galaxy could be suspected from inspection of the frames. The images were recorded in for the most part stable and photometric weather with a mean seeing of ∼0.″75, with typical total integration times (separated into two to five dithered exposures) in R of 1200−2000 s. For a detailed journal of the observations we refer to R96 and Paper I.

The use of broad-band optical filters at the redshifts investigated here results in the inclusion of several prominent emission lines into the filter profiles, most notably [OIII]λ4959+5007, Hα, and Hβ in R and I band. Contributions to these lines can arise from gas ionised by young stars in the host galaxy, from the extended emission line envelopes known to encompass some quasars (mainly steep spectrum RLQ, see e.g. Stockton & MacKenty 1987) and from scattered nuclear light. To make a distinction of the light from the stellar populations in the host galaxies possible, a thorough study of the probable mean sizes of the different flux contributions was made and presented in Paper I. It was found that the corrections to the magnitudes in general are small and do not exceed 0.15 mag for all but three objects. The host galaxy magnitudes presented in this paper have been compensated for the mean influence of the emission lines from envelopes and scattered quasar light.

Our classification of a source as radio-loud or radio-quiet follows the criterion from Kellermann et al. (1989), which for the cosmology assumed in this paper is of the form $L_{5\ \mathrm{GHz}} > 4.5 \times 10^{24}\ \mathrm{W\,Hz^{-1}}$. The existence of the radio-loud/radio-quiet dichotomy was recently disputed by White et al. (2000), who found that the distribution of radio-to-optical flux ratio R for the quasars discovered in the FIRST survey (Becker et al. 1995) did not show the expected bimodality. However, this may be a spurious result as no corrections for selection effects were made, making their sample biased by objects near the flux limit

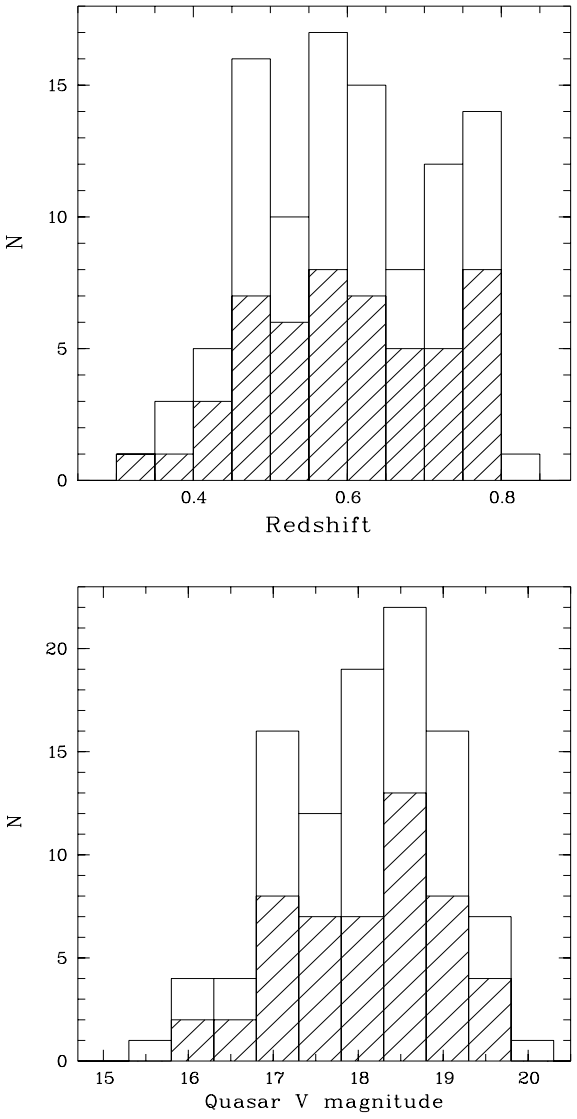

Fig. 1. Histograms of quasar redshift and apparent V magnitude for the combined NOT and NTT samples. The hashed part of the bars marks the data for the radio-loud objects.

as pointed out by Ivezić et al. (2002). The latter authors have cross-correlated the FIRST sources with SDSS (York et al. 2000) and find that the observed R-parameter distribution again suggests bimodality, in agreement with previous work (e.g. Urry & Padovani 1995). The radio properties of the combined NOT and NTT samples (hereafter NON sample) do not indicate the presence of any radio-intermediate objects.

When selecting the NON sample, no attention was paid to the radio spectral index α of the radio-loud sources. In the unified scheme, the flat spectrum (FS) sources are beamed closer to our line of sight than the steep spectrum (SS) sources (e.g. Urry & Padovani 1995), but properties such as large-scale environment and host galaxies should not be affected by orientation. Calculation of the spectral indexes (setting the division between FS and SS objects at $\alpha^5_{2.7} = 0.5$) shows that this resulted in a blind draw of 25 FS and 22 SS sources. Four objects could not be classified.

To ensure that the radio-loud and radio-quiet subsamples were drawn from the same distribution in the z-V plane, a two-dimensional Kolmogorov-Smirnov test was performed. The result confirms that there is no statistically significant difference between the two samples in this respect. In the same way, the FS and SS subsets of the RLQ were also found to be matched.

2.2. Reduction and host galaxy extraction

Data reduction was carried out using the ESO MIDAS package and following standard procedures throughout, with no major differences between the NOT and NTT data sets. During the course of reduction it was found that some sources had to be deselected from the samples because of various problems such as CCD defects or overlapping foreground objects, thus making the NON sample consist of a total of 91 quasars (see R96 and Paper I). The deselection of these sources does not reduce the statistical significance of the matching in the z-V distributions between the RLQ/RQQ and FS/SS subsamples. Of the 91 remaining quasars, 47 are radio-loud and 44 radio-quiet. Four objects from the NOT sample lack photometric calibration.

2.2.1. PSF construction

To extract the properties of the host galaxies, the point spread function (PSF) of the image must be determined. This was done in two different ways: using a purely empirical method and using a combination of empirical and model data. The latter method (described in R96) retains the empirical core but replaces the low signal-to-noise wings with a model, thus extending the residual left after PSF subtraction to fainter flux levels. The central part of the PSF was not replaced since it is difficult to correctly account for the slight non-circularity present due to small tracking errors.

The profile used to model the wings of the PSF was that of Saglia et al. (1993), which analytically approximates observed stellar profiles better than either Gaussian or Moffat functions. The use of a composite PSF produced excellent results for the NTT sample (see R96), but for the NOT sample the method proved to be less satisfactory. This is due to the larger ellipticity of the NOT PSF, which put high demands on the model used for its representation. Thus, although we also applied the composite PSF subtraction method to the NOT data, we preferred to subtract a purely empirical PSF, which simply consists of a suitable field star. Using an empirical PSF to extract a residual leads to a negligible difference in magnitude, compared to the case when a composite PSF is used (see Paper I).

2.2.2. Host galaxy detection

The host galaxy properties were extracted by subtraction of a scaled PSF from the quasar images, where the residual was required to have a flat-top luminosity profile and positive flux at all radii. Such a residual resembles a real galaxy but will correspond to an oversubtraction for elliptical galaxies and spirals with a prominent bulge, since their profiles peak towards the centre. For this reason, the obtained magnitudes must be

regarded as upper limits. Further details of the subtraction process can be found in Paper I.

Host galaxies were detected in a total of 66 sources or 72% of the total NON sample of 91 sources. Of these, 29 are radio-quiet objects (detection rate 66%) and 37 are radio-loud objects (detection rate 79%). For the two classes of radio-loud objects the FS detection rate is 75% and the SS rate is 80%. Comparison of the NOT and the NTT samples shows that the detection rates for radio-loud objects are very similar (80% and 75% respectively), while the rates for radio-quiet objects differ more at 66% and 88%, respectively. The reason for this difference may be the small number statistics, since the radio-quiet NTT subsample in all only consists of nine sources. The limiting magnitude found for the host galaxies in the NON sample was $R = 21.5$ (see R96 and Paper I). Images and luminosity profiles of the resulting host galaxies can be found in R96 and Paper I.

2.3. Error estimation

The two types of errors which can contribute to the host galaxy flux determination are the Poisson error and the systematic oversubtraction which results from the requirement of a flat-top luminosity profile. Since the NTT and NOT samples have been reduced in an almost identical manner, the main difference between them is that for the NOT sample we consistently use magnitudes obtained by subtraction of an empirical PSF while the NTT sample hosts have been recovered using a composite PSF. The latter are therefore not subject to the error introduced from sky variations, which however is small for the NOT data.

The size of the systematical oversubtraction error was estimated in R96 using host galaxy simulations and was after tests found to also apply to the NOT data. For a model galaxy magnitude of $R = 19$, the extracted host flux is less than that of the original object by an amount corresponding to 0.10 ± 0.05 mag, while the difference for $R = 20$ and 21 mag is 0.20 ± 0.10 and 0.50 ± 0.10, respectively.

Comparison in Paper I of magnitudes obtained for objects observed on multiple occasions suggests an error in the subtraction method of around 0.2 mag. Brighter hosts will have magnitudes recoverable by subtraction with an error within 1σ of the total (Poisson) error, whereas faint hosts have a less well-defined magnitude. The Poisson and subtraction method errors in the host galaxy magnitudes thus amount to 0.25−0.3 mag for the objects in the NOT sample and 0.2−0.25 mag for the NTT hosts, to which must be added the systematic oversubtraction error and the K-correction error (see Sect. 4.2 and Tables 2 and 3).

3. The Wold data

An imaging campaign targetting quasars in the redshift interval $0.5 \leq z \leq 0.8$ was carried out in part at the Nordic Optical Telescope by Margrethe Wold, with data taken in 1994, 1996, and 1997. These fields were used to investigate the environments of RLQ and RQQ at intermediate redshifts (see Wold et al. 2000, 2001), but the quality of the data is such that it can also be used for host galaxy analysis. Thanks to the generosity of Dr. Wold and her collaborators we were presented with the reduced field frames obtained by them at the NOT for inclusion in this work.

Of the 16 RLQ and 15 RQQ images we received, nine sources had to be deselected due to various problems such as saturation of the quasar or insufficient alignment of frames before coaddition. In the remaining sample we detected host galaxies in 50% of the RLQ and in 20% of the RQQ. The poor detection rate of radio-quiet objects depends to some extent on the fact that these frames were taken in 1996, where variation of the PSF over the frame was larger than for the 1994 data. It is also of interest to note that re-aluminisation was performed on the NOT mirror in 1995. In general though, the Wold data presented a greater challenge in performing flat-top subtraction due to highly peaked profiles, also leading to lower detection rates.

The eight detected Wold hosts are presented in Table 1, where the exposure times for all frames are 2400 s. The $L_{5\ \mathrm{GHz}}$ fluxes were computed with values taken from the NED database, and all radio-loud objects are steep-spectrum sources. Details of the observations and the reduction can be found in Wold et al. (2000, 2001), but do not deviate by any large degree from the methods used in R96 or Paper I for the objects presented here. Images and luminosity profiles of the Wold sample quasars and host galaxies are presented in Appendix A.

While the reduction was performed by Wold et al., photometric calibration was carried out by us. The photometric error was found to be the same size as in Paper I, i.e. $\lesssim 0.1$ mag. No simulations to test the robustness of the PSF subtraction (carried out using an empirical PSF) were made, but subtraction from field stars left inconspicuous residuals (as for the NON sample, see R96 and Paper I). We will therefore assume that the subtraction errors are of the same order as those derived for the NOT sample. However, the Wold hosts will not be included in the NON sample but will be presented separately in diagrams and statistics.

4. Results and discussion

4.1. Host galaxy morphology

4.1.1. Profile fitting

Most of the hosts in the NON sample are smooth and round or only slightly elongated, though a handful appear somewhat disturbed and a few even display features reminiscent of tidal tails. In order to further determine the morphological properties, galaxy profiles may be fitted to the azimuthally averaged luminosity profiles. At intermediate redshifts this process is highly dependent on the data quality in the outer parts of the profile, where high signal-to-noise ratios are needed to make discrimination of the galaxy type from the wings possible. For the NOT sample, where the ellipticity problem necessitated subtraction of an empirical PSF, galaxy profiles cannot be successfully fitted to the data. In the NTT sample, however, the PSF wings were replaced by models, thus limiting the noise considerably and enabling profile fitting to be carried out.

Due to time and resource constraints, only one-dimensional fitting was performed on the data. In R96 this method was

Table 1. Properties of the resolved Wold sample quasars. Colon signs mark a marginal detection. The *R* band observation of the source 7C 2671 was performed during non-photometric conditions.

Object	α (1950)	δ (1950)	z	$L_{5\ \mathrm{GHz}}$ (10^{26} W Hz^{-1})	Filter	Year	*FWHM* (arcsec)	Quasar (mag)	Host (mag)
MRC 0032–203	00 32 39	−20 20 30	0.518	3.20	*R*	1994	0.88	19.48	19.9:
MRC 0106–233	01 06 38	−23 23 28	0.818	3.09	*R*	1994	0.97	19.14	20.9
					I	1994	0.88	18.71	19.8
MRC 0222–008	02 22 35	−00 49 04	0.687	5.44	*R*	1994	0.79	18.13	20.0
					I	1994	0.62	17.62	19.8:
MRC 0406–180	04 06 52	−18 05 02	0.722	11.1	*R*	1994	0.79	19.16	21.2
7C 2671	10 19 33	45 56 16	0.745	0.87	*R*	1997	0.82		
					I	1997	0.66	18.58	19.1
7C 3066	10 28 48	42 09 46	0.600	0.69	*R*	1994	1.06	18.30	19.4:
BFSP 15152+0244	15 15 16	02 44 02	0.608	–	*R*	1997	0.66	19.47	21.0
BFSP 22011–1857	22 01 09	−18 57 08	0.615	–	*R*	1996	1.23	19.18	20.2
					V	1996	1.06	19.47	20.7

applied to simulated host galaxies and was found to reproduce profile shapes quite well. In general, one-dimensional subtraction methods have been shown to be fairly robust when compared to two-dimensional methods (McLeod & McLeod 2001; Kirhakos et al. 1999; Hooper et al. 1997), with host magnitudes typically differing by no more than a few tenths of a magnitude. The determination of host galaxy morphological types, however, leads to a wider range of results, both when comparing one-dimensional to two-dimensional fitting and when comparing various two-dimensional methods to each other. A common problem is the sensitivity of most methods to the distribution of flux between the nucleus and the host in the central parts, which can lead to the confusion of a peaked profile with an exponential disk.

In the profile fitting analysis of the NTT data set, the morphology could be determined for nine out of 17 sources (see R96 for details). The results show that radio-quiet hosts can be modelled by both spiral and elliptical type galaxies, whereas the radio-loud hosts are almost exclusively better fit by elliptical galaxies. Of the six resolved RQQ host galaxies, one has a firmly determined elliptical profile and two have spiral morphologies, whereas an elliptical profile is the better fit in four of the five resolved radio-loud hosts with clear morphological type determination. The remaining radio-loud host (PKS 1004−217) is better fit by a disk profile, but also displays a clear tidal arm feature.

4.1.2. Axial ratios

For the NOT sample we limited the morphological analysis to determining the axial ratio b/a, which was accomplished by employing the Bender–Möllenhof isophotal ellipse fitting task implemented in MIDAS. The axial ratio was found by computing the mean of the a and b values of the ellipses within the radius determined by the growth curve but excluding the innermost, seeing disk-smeared points. The axial ratio was as a rule very stable over this range, generally varying by not much more than 5−10%.

In Fig. 2 we show the distribution of the axial ratios for the radio-loud and the radio-quiet host galaxies as measured in the *R* band images. The mean value of b/a for the radio-loud hosts is 0.84 ± 0.02, while for the radio-quiet hosts the mean value is 0.85 ± 0.02. The distribution of b/a for the radio-loud objects is somewhat broader than that of the radio-quiet hosts, but not to any significance. The Wold sample quasar host b/a values are not included in the histograms, but the mean (computed for all six objects resolved in *R* regardless of radio loudness) is 0.84 ± 0.05. Figure 2 also shows the axial ratio for a sample of stars. Ten quasar fields were picked at random and the axial ratio determined for all stars in these fields in the same manner as for the galaxies. The stars show, as expected, much larger ratios with the mean $b/a = 0.94 \pm 0.01$.

The resolved NTT host galaxies were also investigated with respect to b/a. The radio-loud hosts have a mean axial ratio of $b/a = 0.83 \pm 0.03$, whereas the mean value of b/a for the radio-quiet hosts is 0.79 ± 0.05. The latter mean is lowered considerably by the value of $b/a = 0.56$ found for the object MC 0415−200, which interestingly enough was classified as a spiral type host in R96. For the two other NTT objects where spiral morphologies were firmly determined in R96, we find $b/a = 0.70$ for the radio-loud host PKS 1004−217 and $b/a = 0.82$ for the radio-quiet host PKS 0958−042, whereas the hosts classified as ellipticals all have $0.82 \leq b/a \leq 0.89$. The number of NTT hosts with morphologies firmly determined by profile fitting is too small to allow a direct statistical comparison to the axial ratios found for the same objects; but as an estimate of the reliability with which axial ratios can be used to evaluate morphological types, the above comparison is encouraging.

The axial ratios of the hosts peak at $b/a \gtrsim 0.8$, in just the same manner as for the normal elliptical galaxy population (Sandage et al. 1970; Lambas et al. 1992). The hosts of both RLQ and RQQ at lower, as well as higher redshift show the same behaviour (Boyce et al. 1998; Dunlop et al. 2003; Kukula et al. 2001), displaying b/a values quite similar to those derived here. Furthermore, the comparison of Schade et al. (2000) of the morphological types of low-redshift hosts to that of the general field population shows that the host galaxies tend to be of earlier type.

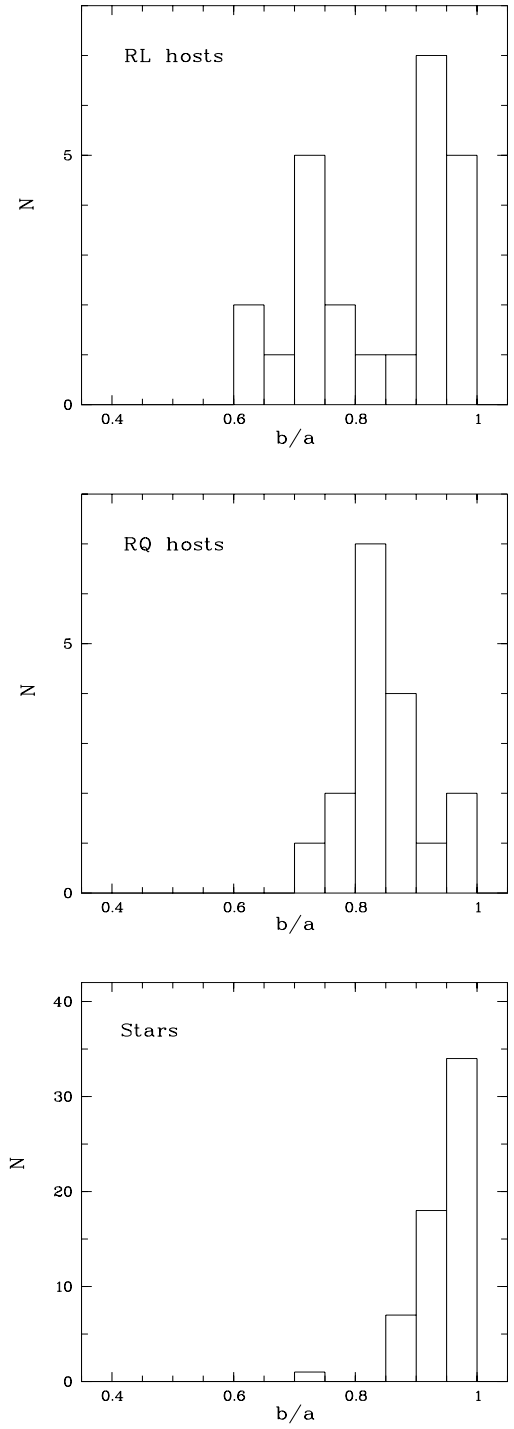

Fig. 2. The axial ratio distribution of the radio-loud and radio-quiet host galaxies in the NOT sample, as well as for a sample of randomly selected field stars. Only resolved objects are included in the histograms.

It is possible that the lack of host galaxies with $b/a < 0.5$ is the result of a selection bias against finding quasars in more inclined disk systems. The higher reddening of the active nucleus for these cases would cause such objects to fall out of UV-excess surveys. A similar deficiency of low axial ratios has also been found for Seyfert 1 galaxies, which are known to be mostly disks (Keel 1980; MacKenty 1990). In addition, Hooper et al. (1997) find much lower axial ratios for a sample at $z \simeq 0.4$ chosen from the LBQS objective prism survey (Hewett et al. 1995), with only two hosts having values higher than 0.6. The reason for this could, however, also be a sensitivity of their modelling to bright features such as tidal tails or bars.

It has been suggested that a limit exists to the quasar luminosity, above which only elliptical hosts are capable of sustaining the activity (McLeod & Rieke 1994; Dunlop et al. 2003). RLQ should, according to Dunlop et al., practically always be found in bulge-dominated hosts due to their higher black hole mass, while lower luminosity RQQ can be hosted by spiral galaxies. In accordance, the hosts with indications of spiral structure in the NTT data are radio-quiet and predominantly belong to the faint half of the sample. However, though the morphology could not be determined for the NOT sample, no dependence of the axial ratio on luminosity is seen for either radio-loud or radio-quiet host galaxies. Exceptions have also been found where bright radio-quiet hosts do show disk-like structure (Percival et al. 2001).

4.2. Host galaxy magnitudes

The resulting Galactic extinction- and K-corrected absolute magnitudes are presented in Table 2 (NOT data) and Table 3 (NTT and Wold data) for the host galaxies and point sources. We used values for the Galactic extinction from Schlegel et al. (1998) for all objects in the sample. Due to the lack of constraints on the internal extinction in the host galaxies no such correction was performed. The magnitudes of the NTT sources observed in the Gunn i band were recomputed to the I band using the relation from Rönnback & Bergvall (1994). Four sources in the NOT sample (Table 2) were not photometrically calibrated, leading us to include only their luminosity ratios in the table.

To be able to K-correct the host magnitudes, we must assume a galaxy type. The optical bands are quite sensitive to K-correction effects which span ~0.5−2 mag in R for intermediate redshifts and also strongly depend on morphological type, differing by as much as a magnitude between elliptical and spiral type galaxies at $z = 0.8$. Thus, the K-correction adds a substantial amount of uncertainty to the estimated absolute host magnitudes, more so at higher redshifts. Further uncertainties are introduced by the varying sizes of the K-corrections found in the literature for the same galaxy classes and by the inclusion of evolutionary effects, which brighten galaxies by 0.5−1 mag over the redshift range studied here (Poggianti 1997).

Investigations at low redshift suggest elliptical galaxies are the dominant host type of both RLQ and RQQ (Dunlop et al. 2003; Schade et al. 2000). With the distribution of axial ratios for the NOT sample clearly favouring elliptical hosts, we adopted the K-corrections for elliptical galaxies from Fukugita et al. (1995) for all NOT and Wold objects. For the NTT sources we used corrections appropriate for the well-determined morphologies from R96, and elliptical galaxy K-corrections for the remaining objects. The galaxy corrections used are shown in Tables 2 and 3 in the column marked "K-corr", where the

Table 2. Absolute magnitudes, errors, and luminosity ratios of the NOT sample objects. Asterisks mark steep spectrum sources, daggers flat spectrum sources, and double daggers objects for which no spectral index could be determined. Colon signs mark marginally resolved sources.

Object	z	$M_{R,\mathrm{nuc}}$	K-corr	ΔK	Host galaxy			Host mag error			$L_{\mathrm{nuc}}/L_{\mathrm{host}}$		
			(R)	(R)	M_R	M_V	M_I	σ_R	σ_V	σ_I	R	V	I
0007+0236	0.59	−22.6	1.19	0.69	−24.0	−23.8	−24.0	0.3	0.4	0.3	1.2	1.9	0.81
0010+0146	0.59										5.2		
0015+1612	0.554	−23.0	1.07	0.62	−23.4			0.3			2.6		
0020–0300	0.58										6.2		
0058+0205	0.599	−23.0	1.22	0.70	−23.4	−24.1	−23.0	0.3	0.3	0.3	3.1	2.9	2.9
PKS 0130+2412⋆	0.457										4.0		
PHL1072	0.615	−23.9	1.28	0.73	−23.6			0.3			6.5		
1E 0136+0606†	0.450	−22.0	0.72	0.42	−22.8		−23.0:	0.3		0.3	1.3		1.3:
KUV 0200–0858	0.77	−25.1	1.80	1.02	−24.8			0.3			10.8		
MC 0212+1708†	0.472	−20.7	0.80	0.46	−22.1			0.4			0.78		
5C6.189†	0.597	−23.0	1.21	0.70	−22.9			0.4			4.7		
EX 0240+0044	0.569	−25.6	1.12	0.65	−24.9	−25.6		0.3	0.3		7.4	6.7	
0256+0140	0.608	−23.3	1.25	0.72	−22.2:			0.6			12.5:		
0305+0222	0.59	−23.8	1.19	0.69	−23.5	−22.4:	−23.7	0.3	1.0	0.3	5.8	21.6:	2.8
PKS 0353+0247⋆	0.602	−24.1	1.23	0.71	−24.6	−24.1	−24.2	0.3	0.6	0.3	2.8	6.3	4.3
3C 138⋆	0.759	−24.4	1.76	1.00	−24.1			0.6			10.8		
GC 0742+3321†	0.610	−22.6	1.26	0.72	−23.4		−23.9	0.3		0.3	2.3		1.0
0929+5319†	0.595	−22.9	1.21	0.70	−23.1			0.4			3.8		
MC 1157+1150⋆	0.731	−23.3	1.67	0.95	−23.9			0.4			4.2		
3C 275.1⋆	0.555	−23.3	1.07	0.62	−23.9	−23.6	−24.3:	0.3	0.3	0.3	2.2	4.6	1.0:
AB122	0.49	−23.4	0.83	0.50	−23.1			0.3			4.3		
E 1332+3730	0.438					−22.3:	−22.9		0.5	0.3		12.7:	3.1
TEX 1423+1438‡	0.78						−23.7:			0.4			1.6:
1435+0130	0.633	−23.6	1.34	0.77	−23.1			0.4			7.7		
PKS 1451+0946†	0.632	−24.3	1.33	0.76	−23.8			0.3			8.2		
B2 1512+3701⋆	0.37	−24.6	0.45	0.27	−22.2:	−22.9		0.3	0.3		16.8:	15.8	
PKS 1530+1342⋆	0.771	−22.7	1.60	0.91	−23.1			0.6			5.3		
PG 1538+4745⋆	0.772	−26.8	1.81	1.03	−25.7			0.3			23.0		
PG 1543+4855	0.40	−24.8	0.55	0.33	−23.7	−22.6	−22.7:	0.3	0.3	0.3	5.8	28.7	14.5:
MC 1548+1129†	0.436	−22.5	0.67	0.40	−21.8			0.4			4.7		
MC 1608+1123⋆	0.457	−21.0	0.74	0.44	−22.0			0.4			1.1		
MS 1640+3940‡	0.540	−23.1	1.02	0.59	−22.7			0.4			4.9		
1640.5	0.625	−21.3	1.31	0.75	−22.9			0.5			1.2		
1641.7	0.705						−22.9			0.4			11.0
1641+3959	0.593	−20.8	1.20	0.69	−23.7	−22.4:		0.3	0.8		0.28	5.5:	
PKS 1819+2249⋆	0.628	−24.6	1.32	0.76	−23.7			0.4			11.5		
4C 40.37⋆	0.733	−24.0	1.67	0.95	−24.3			0.3			5.9		
4C 56.27△	0.664	−23.7	1.44	0.82	−23.5	−23.5:	−24.0	0.4	0.6	0.3	7.1	7.6:	3.3
3C 380⋆	0.692					−26.8	−24.9		0.3	0.3		2.1	5.8
2113+0536	0.509	−21.8	0.92	0.53	−22.7			0.4			1.4		
2141+0402	0.463	−24.6	0.76	0.45	−22.2:			0.4			24.6:		
MC 2142+1101†	0.550	−23.3	1.06	0.61	−23.6		−24.4	0.3		0.3	2.8		0.96
MG2149†	0.52	−24.1	0.96	0.56	−23.8			0.3			4.3		
PKS 2209+0804⋆	0.484	−22.5	0.83	0.49	−22.3	−22.7	−22.9	0.4	0.5	0.3	3.4	2.9	1.6
2217+0845⋆	0.623	−23.1	1.30	0.75	−23.3		−23.3	0.4		0.3	4.2		2.6
2235+0054	0.529	−21.9	0.98	0.57	−22.4			0.4			2.1		
2238+0133	0.714	−24.3	1.61	0.92	−23.9			0.4			10.4		
PKS 2247+1315†	0.767	−23.3	1.79	1.02	−23.7		−23.0:	0.5		0.5	5.6		5.6:
PKS 2351–0036†	0.46										4.1		

column marked "ΔK" tabulates the difference between the K-correction computed for an elliptical and a spiral type host galaxy. In Tables 2 and 3 we also include the individual host galaxy magnitude errors (combining Poisson errors, subtraction method uncertainties, and the systematical oversubtraction error). Nuclear K-corrections were taken from Natali et al. (1998).

In Appendix B we present notes on selected individual objects, where our host magnitudes are compared to those of the few previous studies of the same objects. The properties

Table 3. Absolute magnitudes, errors, and luminosity ratios of the NTT (upper) and Wold sample objects (lower part of table). Asterisks denote steep spectrum sources and daggers flat spectrum sources. The superscripts E and S denote the NTT sources with well-determined morphologies, where K-corrections of appropppriate type were used. Colon signs mark marginally resolved sources.

Object	z	$M_{R,\mathrm{nuc}}$	K-corr	ΔK	Host galaxy			Host mag error			$L_{\mathrm{nuc}}/L_{\mathrm{host}}$		
			(R)	(R)	M_R	M_V	M_I	σ_R	σ_V	σ_I	R	V	I
PKS 0252–549†	0.537	−24.3	1.01^{E}	0.59	−23.6			0.2			7.1		
0314–380	0.484	−24.8	0.83	0.49	−22.5:			0.3			26.3:		
0333–343	0.621	−24.1	1.30^{E}	0.74	−23.9			0.2			6.0		
E 0342–250	0.653	−24.5	1.40	0.80	−22.5:			0.6			32.7:		
PKS 0403–133†	0.571	−24.7	1.13	0.65	−23.4	−23.3	−23.6	0.3	0.4	0.2	12.6	29.5	22.0
MC 0415−200	0.604	−21.8	0.53^{S}	0.71	−22.6			0.3			1.2		
PKS 0920–397†	0.591	−24.8	1.19	0.69	−24.0			0.3			9.2		
PKS 0932+022*	0.652	−24.8	1.40^{E}	0.80	−24.6			0.2			6.7		
MC 0946–197	0.519	−24.2	0.95	0.55	−23.8	−23.8		0.2	0.3		4.9	9.2	
PKS 0958–042	0.497	−23.4	0.37^{S}	0.51	−22.2	−21.9	−23.9:	0.3	0.4	0.3	6.2	11.2	0.22:
PKS 1004–217†	0.330	−23.7	0.12^{S}	0.20	−22.0:	−21.6		0.6	0.4		6.9		
1023–016	0.738	−23.9	1.69	0.96	−24.1	−23.8	−23.9	0.3	0.7	0.3	6.0	11.2	2.9
1025+023	0.745	−23.7	1.71	0.98	−23.5			0.5			9.3		
1045–188†	0.595	−21.9	1.21^{E}	0.69	−23.5	−23.3	−23.6	0.3	0.5	0.2	1.0	3.2	0.32
PKS 1116–462†	0.713	−25.9	1.61^{E}	0.92	−25.2:			0.3			13.1:		
PKS 1156–221†	0.565	−21.2	1.11^{E}	0.64	−23.6	−23.7	−23.6	0.2	0.3	0.2	0.43	1.2	0.31
PKS 1202–262†	0.79	−23.7	1.87	1.06	−24.6:			0.3			4.0:		
MRC 0032–203*	0.518	−21.0	0.95	0.55	−23.1:			0.3			0.49:		
MRC 0106–233*	0.818	−23.3	1.96	1.11	−24.4		−24.4	0.5		0.3	3.9		1.6
MRC 0222–008*	0.687	−24.6	1.52	0.87	−24.3		−23.7:	0.3			8.3		6.6:
MRC 0406–180*	0.72	−23.2	1.63	0.93	−23.5			0.6			5.5		
7C 2671*	0.745						−24.6			0.3	1.4		0.64
0.3 7C 3066*	0.600	−23.2	1.22	0.70	−24.3:			0.3			1.8:		
BFSP 15152+0244	0.608	−22.6	1.25	0.72	−23.0			0.6			3.1		
BFSP 22011–1857	0.615	−22.4	1.28	0.73	−23.6	−23.7		0.3	0.5		1.5	2.2	

Table 4. Mean host galaxy absolute magnitudes of the resolved NON sample.

Type	Band	Mean	# objects
RQ	R	-23.5 ± 0.2	21
RL	R	-23.5 ± 0.2	28
RQ	V	-23.7 ± 0.4	7
RL	V	-23.8 ± 0.5	8
RQ	I	-23.4 ± 0.2	6
RL	I	-23.8 ± 0.2	9
RQ	$R, z \leq 0.6$	-23.4 ± 0.2	12
RL	$R, z \leq 0.6$	-23.1 ± 0.2	16
RQ	$R, z > 0.6$	-23.6 ± 0.2	9
RL	$R, z > 0.6$	-24.0 ± 0.2	12

derived in this paper in general agree quite well with the literature values, whether obtained from ground-based data or the HST.

4.2.1. Mean magnitudes

The mean absolute magnitudes of the resolved NON sample host galaxies are presented in Table 4, where the low-redshift objects PKS 1004–217 and B2 1512+3701, as well as the BL Lac source 4C 56.27, have been excluded from the statistics. Compared to a present-day field galaxy with a Schechter magnitude of $M_R^* = -20.9$ (Lin et al. 1996), the mean values found for the hosts correspond to $\sim 10\ L^*$, similar to the values found in other intermediate redshift studies ($5-12\ L^*$, Hooper et al. 1997; Kotilainen et al. 1998; Kotilainen & Falomo 2000). The difference in mean magnitude between radio-loud and radio-quiet hosts is quite small and less than 1σ (but in the case of I band 2σ).

At low redshifts, many investigations in both optical and near-infrared wavelength bands report fainter mean absolute magnitudes for the galaxies hosting RQQ than for radio-loud hosts, where the size of the difference is ∼0.5 mag (Hooper et al. 1997; Dunlop et al. 2003; Hamilton et al. 2002). As an example, Dunlop et al. find a mean of -22.9 ± 0.1 mag for their radio-loud objects, while the radio-quiet objects have a mean of -22.4 ± 0.2 mag (with their R band values converted to the cosmology used in this paper). When turning to redshifts >0.5 but lower than unity, very few observations of radio-quiet host galaxies exist. The mean magnitudes of radio-loud hosts have grown brighter by ≲0.5 mag; Márquez et al. (1999) find a mean of -23.0 ± 0.4, while Kotilainen et al. (1998) derive a mean of -23.1 ± 0.5 for FS host galaxies and -23.6 ± 0.3 for SS hosts (Kotilainen & Falomo 2000), where quoted magnitudes have been recomputed to the R band and the cosmology of this paper.

In Fig. 3 we show the distribution of absolute host galaxy R magnitudes with redshift for the NON and Wold sample

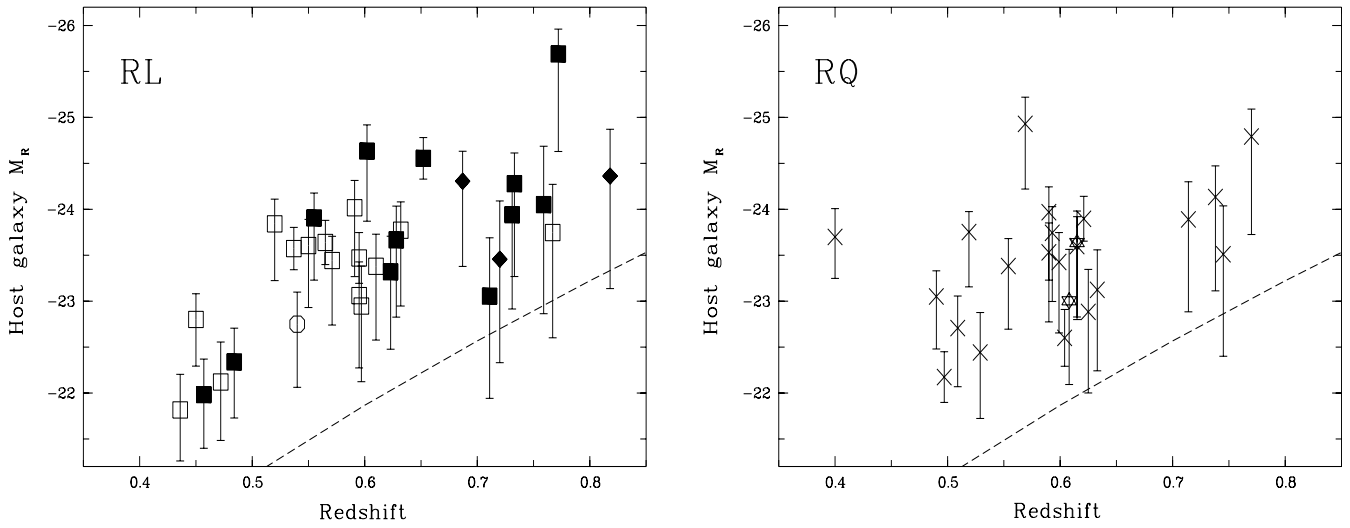

Fig. 3. The distribution of host galaxy magnitudes with redshift. Only resolved objects were included. *Left panel*: radio-loud objects. Filled squares mark NON sample SS sources, empty squares NON sample FS sources, and filled diamonds Wold sample SS objects. Circles mark radio-loud objects in the NON sample for which no spectral index could be calculated. *Right panel*: radio-quiet objects. Crosses mark NON sample data and stars Wold sample data. The dashed line marks the absolute magnitude corresponding to the NON sample detection limit of $R = 21.5$ mag. The error bars are asymmetrical due to the inclusion of the uncertainty in the K-correction.

objects. The error bars are asymmetric, as they include the K-correction uncertainty (present for all objects except the NTT sources with well-determined morphologies), which can be seen to increase substantially with redshift. Note that even with the inclusion of the ΔK, all but a handful of sources are still well above the detection limit. Dividing the sample into two parts to further investigate the redshift dependence of the mean magnitudes (see Table 4) results in a radio-loud mean host magnitude at lower redshift, which is fainter than that found for the radio-quiet hosts (at the 1.5σ level), while the reverse is true for the upper redshift range (at the 2σ level). In other words, the mean magnitudes of the radio-loud hosts tend to grow brighter at higher redshifts, while the radio-quiet hosts on the other hand show more similar brightness over the range. A Spearman rank test shows that the radio-loud host absolute R magnitudes are correlated with the redshift at a significance level $p < 0.005$, but also that the radio-quiet host magnitudes are weakly correlated with redshift ($p < 0.05$).

In Fig. 4 data taken from several samples from the literature have been transformed to the R band and converted to the cosmology used in this paper. To transform the V band observations of Boyce et al. (1998) and Hamilton et al. (2002) $V - R = 0.8$ was used (Fukugita et al. 1995). The data sets of Kotilainen et al. (1998), Kotilainen & Falomo (2000), and McLeod & McLeod (2001), which were obtained in the H band, that of Márquez et al. (1999) who observed in the J band, and the K band data of Percival et al. (2001) were recomputed by combining optical and near-infrared-to-optical colours from Fukugita et al. (1995) and Poggianti (1997), resulting in $R - H = 2.2$, $R - J = 1.4$ and $R - K = 2.5$. All colour relations assume an elliptical host galaxy morphology.

When comparing the two panels in Fig. 4, the ∼0.5 mag offset between the mean absolute magnitudes of radio-loud and radio-quiet hosts at low redshift is immediately clear, as is also the paucity of literature data for radio-quiet hosts at $z > 0.4$. The radio-loud NON sample objects span a magnitude range very similar to that of the literature data, but the radio-quiet hosts are brighter in comparison. However, the overlap in redshift is quite small for the radio-quiet objects, with the NON sources sampling higher redshifts. There is also the suggestion of an upturn in host magnitude at $z \gtrsim 0.5$, both for radio-loud and radio-quiet objects.

By obtaining data for host galaxies at $z \sim 0.2, z \sim 1$, and $z \sim 2$, Kukula et al. (2001) have investigated the evolution of host luminosities. For radio-loud hosts they find an increase in luminosity with redshift, which is consistent with that expected from simple passive evolution of massive spheroids (see also Falomo et al. 2001). The radio-quiet hosts, however, seem little changed in luminosity over the redshift range, with luminosities which only reach $\simeq L^*$ at $z \sim 2$ (Ridgway et al. 2001). Radio-quiet hosts as bright as the most luminous radio-loud hosts have, however, also been detected at these redshifts (Aretxaga et al. 1998; Hutchings et al. 2002). As argued by Kukula et al. and Dunlop et al. (2003), the difference between the high-redshift radio-loud and radio-quiet hosts is suggestive of different evolutionary scenarios for radio-loud and radio-quiet objects, where the radio-loud hosts are already fully assembled at $z \sim 2$. Since the radio-quiet hosts are fainter at these high redshifts than expected from passive evolution, it seems possible that mass acquisition can take place at lower redshifts for these objects, making them significantly different from their radio-loud counterparts.

The radio-loud objects in this study are consistent with the evolutionary scenario proposed by e.g. Kukula et al. in that they grow brighter from the low to the high redshift ends of the sample, connecting to the low-redshift objects from the literature and extending towards the brighter sources found at $z \sim 2$. The radio-quiet hosts also conform to expectations by remaining

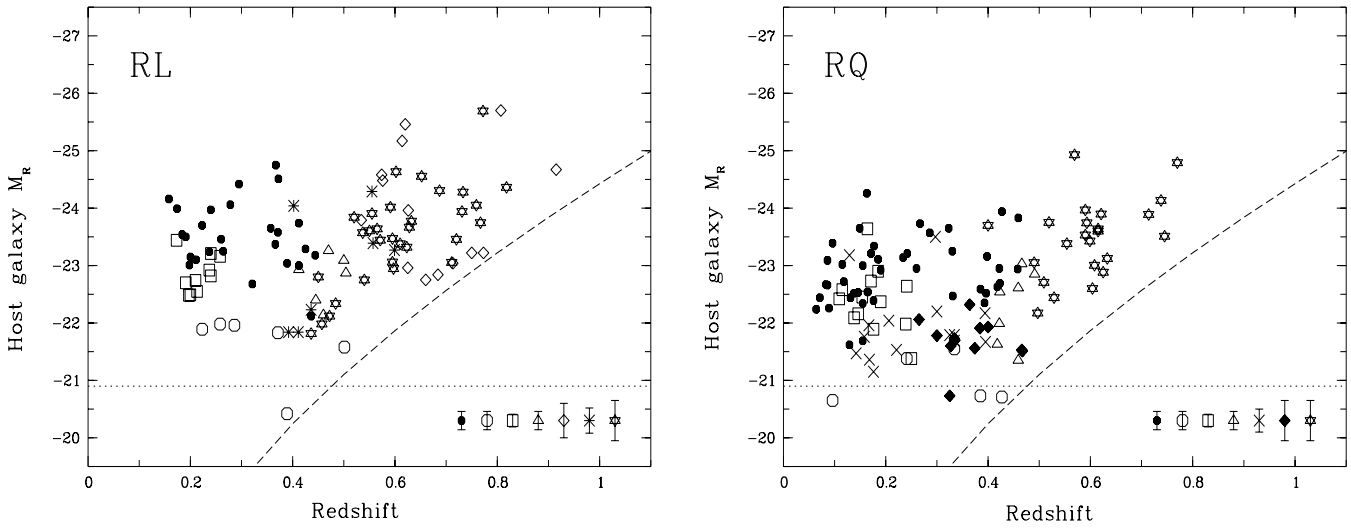

Fig. 4. The distribution of host galaxy magnitudes with redshift. *Left panel*: radio-loud objects. Stars mark NON+Wold sample sources, where only resolved objects have been included. Solid circles mark data from Hamilton et al. (2002) and empty circles data from Boyce et al. (1998); squares mark data from Dunlop et al. (2003) and triangles objects from Hooper et al. (1997); diamonds mark resolved data from Kotilainen et al. (1998) and Kotilainen & Falomo (2000); asterisks mark objects taken from Márquez et al. (1999). *Right panel*: radio-quiet objects. Symbols as for the left panel except for crosses, which mark data from McLeod & McLeod (2001) and filled diamonds, which mark data from Percival et al. (2001). The dotted line shows the location of a present-day L^* galaxy ($M_R^* = -20.9$, Lin et al. 1996), and the dashed line marks the absolute magnitude corresponding to the NON sample detection limit. At lower right the typical 2σ systematical host galaxy magnitude error bars are shown for the various samples.

similarly bright over the redshift range investigated, but they deviate from the low-redshift studies by having a mean magnitude similar to that of the radio-loud hosts.

It must be noted that a number of effects can influence the tentative magnitude trends discussed here. The difficulty in assigning proper K-corrections may introduce a systematic error which could affect the similarity between the mean radio-loud and radio-quiet host magnitudes. The size of this error is redshift-dependent, since the difference between K-corrections for different galaxy types increases with redshift. If the morphological types of the two populations differ more than has been assumed here so that a higher fraction of the RQQ have disk hosts, the faulty K-correction for these objects will force them to brighter magnitudes and lower the mean. Should, for instance, half of all NON RQQ reside in disk hosts, the mean radio-quiet host magnitude would be fainter by ∼0.25 mag, which however still is less of a difference than found in the literature between low redshift radio-loud and radio-quiet hosts. The blue colours of the hosts (see Sect. 4.3) can also affect the magnitude values, since too large a K-correction will be assumed for an object which has a larger luminosity at shorter wavelengths than a normal galaxy of the designated Hubble type.

From these results it is clear that a well-determined K-correction is of vital importance when investigating the absolute magnitudes of quasar hosts over the intermediate redshift range. To lessen the influence from this source of uncertainty, observational data is needed which either is of good enough quality for the morphology to be confidently determined, or is obtained by employing different filters so that a similar region in the host galaxy spectrum is always sampled irrespective of redshift. A third method would be to use several filters in order to properly sample the spectral energy distribution of the hosts.

Without any K-correction applied, the distribution of apparent magnitude with redshift for the radio-quiet hosts is indistinguishable from that of the radio-loud hosts, as found from the two-dimensional Kolmogorov-Smirnov test performed in Paper I. The brightening with redshift of the radio-loud hosts is also seen in the non-K-corrected data, but the correlation is less significant (a Spearman rank test yields $p < 0.01$). However, since the NON sample is not fully resolved (nor are the samples of Kotilainen et al. 1998 and Kotilainen & Falomo 2000, which form the other large samples of intermediate redshift quasars), the upturn, as well as the increase of host magnitude with redshift, might be a result of the larger volumes sampled. The relationship between host and nuclear luminosity and the increasing difficulty of resolving faint hosts (as evidenced by the sample detection limit in Figs. 3 and 4) would then conspire to produce a relationship between host magnitude and redshift though only an upper limit is detected.

4.2.2. Luminosity ratios

In Tables 2 and 3 the nucleus-to-host galaxy luminosity ratios of the NON and Wold sample are also presented. A comparison of the ratios obtained for the same object, but in different wavelength bands, shows that these do not differ by any large amounts. In general, R and V band ratios only differ by a factor 0.5−1, while the difference between R and I bands is slightly larger at a factor 1−3. The hosts are thus at their weakest compared to the nuclear light in the V band and grow progressively brighter through R and I band, which is broadly

consistent with the increasing significance of quasar light at shorter wavelengths. There is no significant difference between the luminosity ratios of resolved radio-loud and radio-quiet hosts in any of the bands investigated.

In the study performed by Kotilainen et al. (1998) and Kotilainen & Falomo (2000) on FS and SS RLQ, respectively, it was found that the luminosity ratios differ markedly between the two types of quasar. The core-dominated FS sources in their sample had a mean luminosity ratio of 21 ± 3, whereas the lobe-dominated SS sources had a mean ratio of 3.8 ± 1.1. The mean ratio for the FS objects includes marginally resolved objects: if the corresponding value is calculated including only resolved objects, the ratio sinks to 9.7 ± 3.1. No major difference was found between the host galaxy mean magnitudes of the two samples, but the nuclear component of the SS objects was on average ∼1.5 mag fainter than that of the FS sources. This fits well with the unified scheme, where the core-dominated quasars are beamed closer to our line of sight than the SS sources and thus, as a natural consequence, have higher ratios of nuclear to host light.

Examining the NON+Wold sample in this respect yields a mean luminosity ratio of the FS objects which is 4.4 ± 0.9. The mean of the SS objects is slightly higher at 6.6 ± 1.4 (but only at the 1.5σ level), in contrast to the previous findings. We also computed the mean luminosity ratios for the low redshift radio-loud objects in the sample of Hamilton et al. (2002). For the FS objects in this study we find a value of 2.8 ± 0.7, while the SS sources have a mean of 3.0 ± 0.6. Thus no effect of beaming is seen in either of these samples.

4.2.3. The host-nucleus luminosity limit

A trend between host galaxy magnitude and point source brightness was noted by e.g. Véron-Cetty & Woltjer (1990) and McLeod & Rieke (1995), in the sense that there seems to exist a minimum host galaxy luminosity which increases with nuclear luminosity, indicating that a more massive host is required to sustain a brighter quasar. This can be interpreted as an extension of the correlation found for local ellipticals between black hole mass and bulge luminosity (Magorrian et al. 1998; Merritt & Ferrarese 2001) to quasar host galaxies. The correlation has also been observed for quasar hosts (Laor 1998; Ferrarese et al. 2001; McLure & Dunlop 2002; Wandel 2002), and can be translated into an upper limit to the constant fraction of the Eddington luminosity at which the quasar radiates.

There are two selection effects which could influence the distribution of data points over the host galaxy-nuclear luminosity plane. The lower right corner contains faint galaxies hosting bright quasars and could suffer from a lack of data points due to the larger difficulty in resolving such sources, whereas faint AGNs in bright galaxies run the risk of falling out of quasar catalogues and hereby depopulating the upper left corner.

In Fig. 5 the magnitudes of the NON and Wold sample hosts are plotted against nuclear magnitude. The lines mark the 1% and 10% ratio of Eddington luminosity ($L/L_{\rm Edd}$) and were recalculated to R band from the expression used in

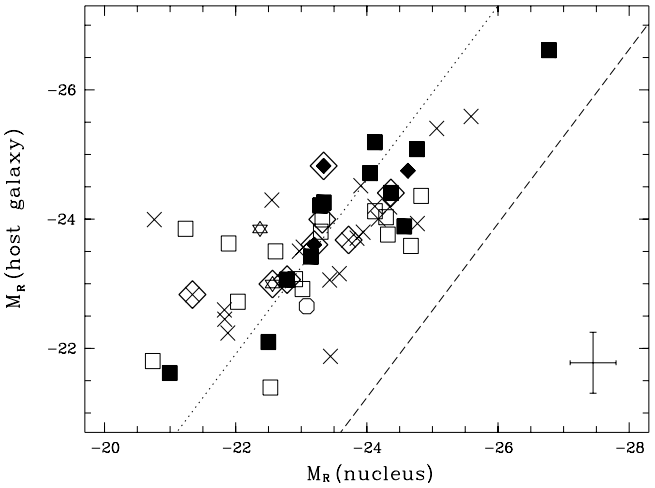

Fig. 5. Host galaxy vs. nuclear absolute magnitudes. Only resolved objects have been plotted, with symbols as in Fig. 3. The mean 2σ systematical magnitude error bars are shown in the lower right corner. The eight symbols enclosed by a diamond have individual error-bars larger than 0.45 mag (1σ above the mean magnitude error). The dashed line marks an Eddington ratio of $L/L_{\rm Edd} = 0.1$, and the dotted line marks $L/L_{\rm Edd} = 0.01$.

McLeod et al. (1999). As can be seen in Fig. 5, there is a tendency for brighter quasars to reside in more luminous host galaxies, regardless of radio properties. A weighted fit to the data results in a relation which is flatter than that given by any single Eddington ratio (for which the fit results in a reduced $\chi^2 = 3.1$) and which is dominated by the objects with the brightest nuclei. There is a dependency on redshift for the objects in Fig. 5 in the sense that objects with higher redshift tend to have both higher nuclear and host luminosity than lower redshift sources.

The upper bound of the distribution in Fig. 5 is consistent with objects which radiate at an Eddington ratio of ∼5%, but the mean of the sample is much lower at a ratio of 1.5% ± 0.9%. Though this is well below the limit of $L/L_{\rm Edd} \leq 20\%$ found for bright low redshift quasars by McLeod & McLeod (2001), it is in agreement with the typical ratios of objects at both low redshift ($z < 0.15$, rate < 5%, Schade et al. 2000) and somewhat higher redshift ($z < 0.5$, rate < 5% calculated from the data of Hooper et al. 1997) but not with the ratios of objects at $z \sim 0.7$, which are consistent with the upper limit of 20% found by McLeod & McLeod (Kotilainen et al. 1998; Kotilainen & Falomo 2000).

The difference between the upper bounds found for the NON and Wold sample and the samples of Kotilainen et al. could perhaps be caused by the fact that their investigations were performed in the H band. Since the contrast between nuclear and host light is more favourable in the near-infrared than in the optical, this could increase their detection rate for bright objects hosted by faint galaxies.

4.3. Host galaxy colours

In Table 5 we present the colours of the NON and Wold sample quasars and host galaxies, computed for resolved objects only. The colours of the NTT sources were tabulated in R96, but are

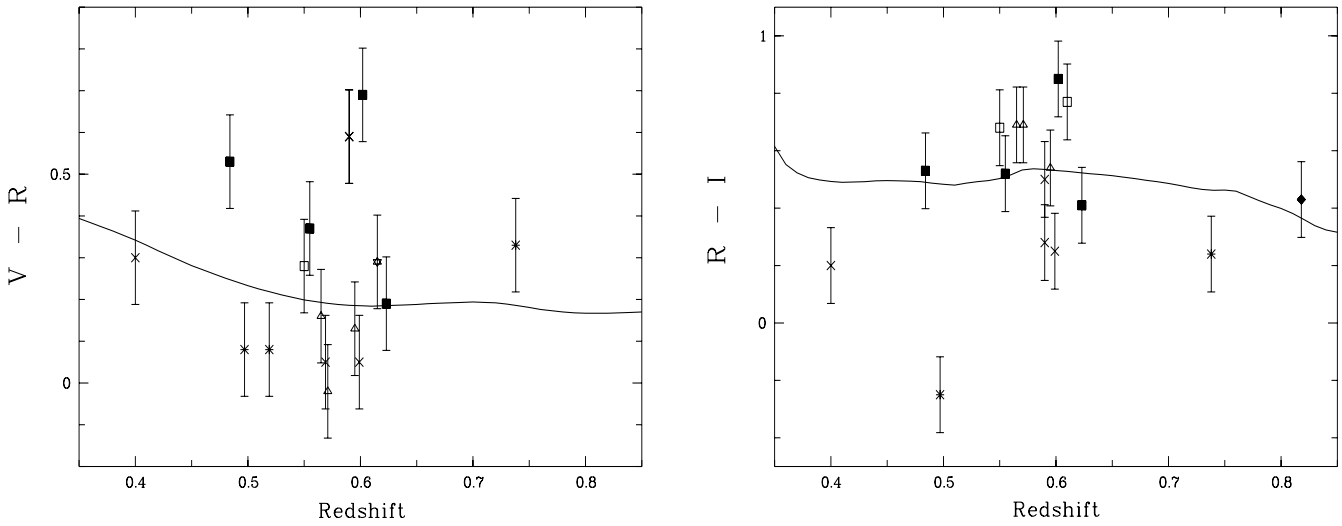

Fig. 6. Quasar colours. Filled squares mark NOT sample SS sources, empty squares NOT sample FS sources and crosses radio-quiet NOT objects. NTT FS sources are marked by empty triangles and radio-quiet NTT objects by asterisks. Wold sample SS sources are shown by filled diamonds and radio-quiet objects by stars. The solid lines mark the colours of the composite quasar spectrum of Vanden Berk et al. (2001), which were computed by integrating the redshifted filter profiles convolved with the quasar spectrum.

Table 5. Colours of the resolved NON and Wold sample objects, obtained from full aperture measurements.

Object	z	Quasar		Host galaxy	
		$V-R$	$R-I$	$V-R$	$R-I$
0007+0236°	0.59	0.59	0.50	0.9	0.8
0058+0205°	0.599	0.05	0.25	0.1	0.4
MRC 0106–233$^{\star\,\circ}$	0.818		0.43		1.1
EX 0240+0044	0.569	0.05		0.0	
0305+0222	0.59	0.59	0.28		1.0
PKS 0353+0247$^{\star\,\circ}$	0.602	0.69	0.85	0.4	0.9
PKS 0403–133$^{\dagger\,\circ}$	0.571	−0.02	0.69	0.86	0.86
GC 0742+3321†	0.610		0.77		1.4
MC 0946–197	0.519	0.08		0.67	
PKS 0958–042	0.497	0.08	−0.25	0.71	
1023–016°	0.738	0.33	0.24	0.98	0.78
1045–188†	0.595	0.13	0.54	0.91	0.84
PKS 1156–221†	0.565	0.16	0.55	0.63	0.63
3C 275.1*	0.555	0.37	0.52	1.0	
PG 1543+4855°	0.40	0.30	0.20	1.9	
MC 2142+1101†	0.550	0.28	0.68		1.2
BFSP 22011–1857	0.615	0.29		0.6	
PKS 2209+0804*	0.484	0.53	0.53	0.5	1.2
2217+0845*	0.623	0.19	0.41		0.8

* Steep spectrum source.
† Flat spectrum source.
$^{\circ}$ Odd or disturbed morphology.

shown here recalculated from $R-i$ to $R-I$. The BL Lac source 4C 56.27 has again been excluded from tables and plots, but is discussed in detail in Sect. B.9.

To investigate the quasar colours as a function of redshift, we have integrated the redshifted filter profiles convolved with the composite quasar spectrum obtained from the SDSS (Vanden Berk et al. 2001). The result is shown in Fig. 6 together with the quasar data, which in general agree well with the colours of the composite quasar. We note that the RLQ are redder in $R-I$ than the RQQ, with mean colours of $R-I = 0.60 \pm 0.05$ and 0.20 ± 0.10, respectively, which could indicate a higher fraction of host galaxy contamination for the RLQ.

A comparison of the host galaxy colours in Table 5 to those of the quasars reveals that the former are redder in almost all instances, as expected if the host light mainly is due to stellar emission. Four objects make an exception in this respect: 0058+0205, EX 0240+0044, PKS 0353+0247, and PKS 2209+0804. The blue colours of these sources could be caused by young stars in a starburst, but also by scattered continuum light from the nucleus in analogy with the situation in radio galaxies. However, while scattered light can make a substantial contribution to the ultraviolet continuum emission in radio galaxies, less is known of its role in quasar host galaxies. By comparing radio galaxies and RLQ, it has been estimated that the fraction of scattered light is on the order of ∼10% of the total nuclear light (Fosbury 1997).

In studies of radio galaxies, it seems likely that the main scattering agent is dust (Cimatti et al. 1996; Dey et al. 1996). Current models of radiative transfer in an inhomogeneous dusty and clumpy medium show that the dust will give rise to an overall grey scattering, given that it has the same properties as Galactic dust (Witt & Gordon 1996, 2000; Városi & Dwek 1999). The scattering process will not, therefore, in itself cause a blueing of the light, but will only result in an additional flux component contributing to the host flux in different filters depending on the redshift of the object. The prominence of the scattered light fraction will be larger at shorter wavelengths where the AGN light dominates, thereby mainly influencing the V band, though the R band also begins to be affected at $z > 0.5$. Note, though, that only 30% of the objects in a complete sample of radio galaxies at redshifts up to $z \leq 0.7$ show

Table 6. Annular colours of resolved NON and Wold sample objects which differ by >0.1 mag from colours measured in a full aperture. The asterisk marks a steep spectrum source.

Object	z	Host galaxy	
		$V-R$	$R-I$
0305+0222	0.59		1.2
PKS 0353+0247⋆	0.602	0.9	0.5
PG 1543+4855	0.40	1.6	

a significant contribution of scattered light to the UV excess (Tadhunter et al. 2002).

To investigate the importance of scattered nuclear light, we measured the colours of all hosts in an annular aperture extending between the seeing disk and the asymptotic growth curve limit. For most sources the difference between full and annular aperture colour is <0.1 mag, but for the three objects listed in Table 6 the difference varies between 0.2−0.5 mag. In general, the annular colours are redder than the full aperture colours. The bluer annular colour of the object PG 1543+4855 is in all likelihood connected to the evidence of strong interaction and a recent starburst found by Canalizo & Stockton (2001, see Sect. B.6). Of the four previously mentioned objects which had very blue full aperture colours, three have annular colours redder than that of the quasar. However, no change is seen for EX 0240+0044. The annular colour of both this source and of PKS 0353+0247 in $R-I$ are still bluer than that of the corresponding quasar.

Note also that when inspecting the images of the objects in Table 5 (see R96, Paper I and Fig. A.1 in this paper), it can be seen that a sizeable fraction has close companions in projection (∼65%), and some even exhibit visibly disturbed morphologies. The objects in Table 6 all show these traits, and the sources PKS 0353+0247, as well as 0058+0205, also seem to be in interaction. A large population of young stars as an explanation for the blue full aperture colours of these hosts is therefore not unreasonable, though contributions from scattered nuclear light cannot be ruled out. This especially holds in the case of EX 0240+0044, which has a featureless host in both the R and the V band image. The morphology of this host shows no obvious signs of recent interaction which could trigger star formation and lead to a bright V band image. This may, however, simply be due to unfavourable projection on the sky or because the merger is old enough that the morphological change is complete. In general, the small difference between full and annular aperture colours for the majority of the objects indicates that the colours of the host galaxies are not affected by scattered nuclear light.

In Fig. 7 the host colours are plotted as a function of redshift, where we show the annular colours for all objects. The sources from Table 6 together with those objects which had a full aperture colour bluer than that of the quasar are marked by encircled symbols since these values are subjected to above-average uncertainties. The colours of the template galaxy spectra shown in Fig. 7 were derived by integrating the redshifted filter profiles convolved with spectral energy distributions adopted from Kinney et al. (1996). SB1 and SB6 identify two different classes of starburst galaxies taken from Calzetti et al. (1994). These are grouped according to the values of their intrinsic colour excess, where SB1 and SB6 represent the extreme ends of the distribution at $E(B-V) = 0.05$ and $E(B-V) = 0.65$, respectively.

Table 7. Mean colour relations of the resolved NON sample.

Type	Colour	Mean	# objects
RQ	$V-R$	0.77 ± 0.07	5
RL	$V-R$	0.82 ± 0.07	4
RQ	$R-I$	0.66 ± 0.08	3
RL	$R-I$	0.99 ± 0.09	7

The $V-R$ host galaxy colours are even within the errors mainly as blue as those of present-day late-type spirals. This could in part be caused by the larger difficulty of detecting red hosts in the V band, which leads to a deficiency of such objects in the z vs. $V-R$ colour diagram. Turning to the $R-I$ colour, the situation is indeed not as distinct: some objects have colours which, within the errors, are similar to E or S0 type galaxies, though the large majority of sources are at least as blue as an Sb galaxy also at these wavelengths. The two objects redder than an Sb galaxy in $R-I$ which have a magnitude difference <0.1 between the full and annular aperture colour are further discussed in Sect. B.3.

For the NTT sources with well-determined morphology, we find that the elliptical type hosts are positioned in the same parts of Fig. 7 as the spiral type hosts. The effect of galaxy evolution over the redshift range is to make the galaxy template colours bluer than shown in Fig. 7, but the general size of the colour shifts are not more than ≲0.2 mag (Poggianti 1997), which does not change the above conclusions.

The mean colours of the radio-loud and radio-quiet sources are shown in Table 7, computed using only the sources with similar full and annular aperture measurements. There is no significant difference between the mean $V-R$ colour of the radio-loud and radio-quiet hosts, but the mean $R-I$ colours differ by $\sim 4\sigma$. It is tempting to interpret this difference as an indication for redder RLQ hosts, but no firm conclusion can be drawn given the small sample sizes. The $V-R$ colours of the hosts in this study are in the mean ∼0.7 mag bluer when compared to the colours of template normal elliptical galaxies at the same redshift, while the mean difference in $R-I$ for the total sample is ∼0.6 mag.

4.4. Comparisons to host colours derived in other investigations

Few studies of quasar host galaxy colours exist even at low redshift. The greatest effort by far has been made by Jahnke et al. (2004), who performed imaging in seven bandpasses (B, V, R, i, J, H, and K) for a sample of 19 objects at $z < 0.2$. The obtained colours are bluer than those of normal inactive galaxies both for short and long wavelength baselines. In particular, the hosts classified as elliptical galaxies are as blue as intermediate to late-type spirals, which contrasts to the results of Dunlop et al. (2003), who find $R-K$ colours at $z < 0.25$,

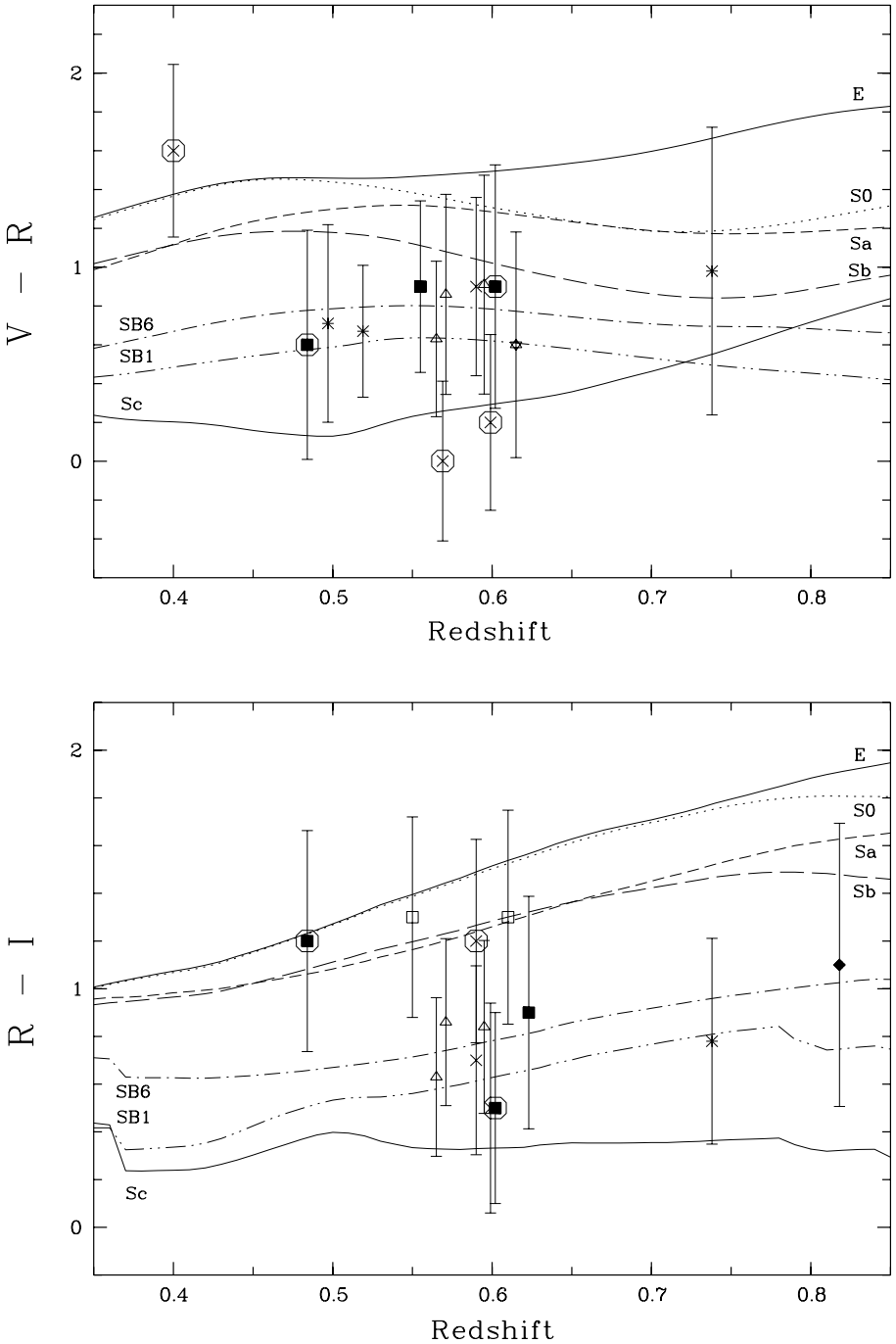

Fig. 7. Host colours (measured in an annular aperture) as a function of redshift. Filled squares mark NOT sample SS sources, empty squares NOT sample FS sources, and crosses radio-quiet NOT objects. NTT FS sources are marked by empty triangles and radio-quiet NTT objects by asterisks. Wold sample SS sources are shown by filled diamonds and radio-quiet objects by stars. The encircled symbols mark the objects which have an annular aperture magnitude differing from that of the full aperture by >0.1 mag or have a full aperture colour bluer than that of the quasar. The lines represent the colours of present-day galaxies of different Hubble types, derived from template galaxy spectra by integrating the redshifted filter profiles convolved with spectral energy distributions adopted from Kinney et al. (1996) and Calzetti et al. (1994).

which are very similar to those of massive, well-evolved ellipticals formed at high redshift ($z > 2$).

Colour information is even scarcer at $z > 0.3$. Only a handful of studies have been published to date, and are discussed in the following. The colours found in these studies are quite blue, often as blue as those of an Sb-Sc galaxy and in some instances even bluer. A notable exception is the very red host of the object detected by Brotherton et al. (2002) at $z = 0.634$, which contains both an AGN and a nuclear starburst.

Romanishin & Hintzen (1989) find a $V - R$ of 0.87 ± 0.15 for a source at $z = 0.411$, consistent with the colours of an Sb galaxy and very similar to what is found for the NON sample. Colours were also obtained by Véron-Cetty & Woltjer (1990) in $R - i$ for six objects in the range $0.31 < z < 0.43$,

of which only one source is radio-quiet. These authors measure the magnitudes in an annular aperture of fixed metric size, well removed from the nucleus at 12.5 − 25.0 kpc. They find a mean colour of $R - i = 0.02 \pm 0.24$, which when transformed to $R - I$ results in a mean value of 0.77 ± 0.24, which is closer to the typical colour of an Sb galaxy than of an elliptical.

Using the HST, Kirhakos et al. (1999) determined the colours of the hosts of three RLQ at $0.36 < z < 0.60$, which are bluer in $V - I$ by 1−1.5 mag compared to the predicted value for an elliptical galaxy at these redshifts. Their highest redshift source (at $z = 0.594$) has a $V - I$ colour of 1.3, while the mean of the five well-behaved NON sources with images in both V and I is 1.3 ± 0.3, four of which are located at $0.55 < z < 0.65$. Kirhakos et al. also measured the colours in an annular aperture and found an average difference to their full aperture colours of only 0.13 mag, again leading to the conclusion that scattered nuclear light is not affecting the blue colours of the hosts by any large amount.

Sánchez et al. (2004) also recently used the HST to derive the F606W − F850LP colour for the hosts of 15 quasars (for which no radio luminosities were given) at $0.5 < z < 1.1$. The host galaxies showed a wide range of colour indicative of the presence of different stellar populations, but ∼50−70% of the hosts classified as early-type were found to be distinctly blue when compared to inactive galaxies at $z \sim 0.7$ taken from Bell et al. (2004). Even when the blue tail of early-type galaxies (see below) is taken into account, the colours remain significantly bluer for the most luminous sources. The colour data is compared by these authors to the models of Bruzual & Charlot (2003), and is found to be well fit both by single stellar populations having a mean age of ∼1 Gyr and by mixes of an underlying old population together with a small mass fraction of young stars (from close to 0% to 30%).

With regard to the colours of non-active galaxies, a population of blue early-type galaxies at $z < 1$ have in recent years been identified in HST surveys. These make up between 15−40% of the total number of E/S0 galaxies, where at least some objects at higher redshifts have luminosities similar to those of standard red ellipticals (Menanteau et al. 1999; Schade et al. 1999; Abraham et al. 1999; Im et al. 2001; Bell et al. 2004). The blue colour is for blue objects at lower redshift often concentrated towards the central region, while the exterior parts have the same colour as red early-type galaxies (Im et al. 2001; Menanteau et al. 2004). The last group of authors also find that the fraction of systems displaying a pronounced colour gradient is almost constant up to $z \leq 1.2$. Cross et al. (2004) have studied elliptical galaxies at $0.5 < z < 1.0$ and find that, while blue ellipticals are smaller than their red counterparts at fainter magnitudes, there are no differences in the average sizes or Sersic parameters between red and blue galaxies, which are brighter than $M_B < -20.1$. Fitting by Cross et al. of Bruzual & Charlot (2003) models to the overall colours also indicates that the bright blue ellipticals have higher current star formation rates, which seems to occur preferentially in the cores of these galaxies.

Considerable circumstantial evidence, such as tidal tails and asymmetries in the host galaxies, extended emission, and close companions, favour the idea that strong interactions can provide the means to transport material to the centre of the host galaxy, where it can trigger and fuel the active nucleus, as well as star formation (see e.g. Stockton 1990; Hutchings & Neff 1992; Hutchings & Morris 1995; Boyce et al. 1996; Bahcall et al. 1997). The hosts of the NON and Wold sample objects frequently have projected close companions and a few display asymmetries or even tail-like features not expected of ellipticals. Interaction or merging leading to ongoing star formation is thus a viable explanation for the blue colours of the hosts. Even bright featureless hosts like EX 0240+0044 (see Sect. 4.3) might simply be examples of active counterparts to the non-active blue elliptical population discussed by e.g. Cross et al. (2004), as ∼70% of the quasar host galaxies presented here are bright enough to fall below their $M_B < -20.1$ limit (transforming from R to B using the colour relation for elliptical galaxies from Fukugita et al. 1995), including EX 0240+0044 itself.

Two important selection biases in the NON sample must be noted. First, since the imaging was performed in filters which at these redshifts include [OII]λ3727, [OIII]λ5007, Hα, or Hβ, the observations are more sensitive to host galaxies with a pronounced young stellar population. However, the influence of these emission lines was shown in Paper I to probably not be very important. Second, the only NTT sources for which multiple band imaging was performed were those which at the telescope indicated a host. This selection effect also applies to the NOT sample, though for these frames the process included crude reduction performed during the day. Only the Wold sample which was not aimed at host galaxy detection is free from this bias, but it forms a minority of the objects. Therefore, the colour analysis results are valid for host galaxies which are large, bright, have low nucleus-to-host luminosity ratios, and/or display large scale disturbances, but cannot safely be generalised to hold for the quasar host galaxy population at intermediate redshifts as a whole. Note, however, that the objects studied with respect to colour were evenly distributed over the quasar luminosity range of the NON sample.

While the results from studies of broad-band colours mainly suggest hosts as blue as late-type spirals and starburst galaxies at both low and intermediate redshifts, this method is a blunt tool with which to investigate the composition and ages of stellar populations: for these purposes spectral information is to be preferred. Very few such studies of host galaxies exist, and only at $z < 0.25$. Hughes et al. (2000) obtained off-nuclear spectra of a subset of the hosts studied by Dunlop et al. (2003). The analysis (see Nolan et al. 2001) showed that evolved stars with ages of 6−14 Gyr dominate the hosts, which is consistent with the broad-band colour result of Dunlop et al. Jahnke (2002) instead utilised two-dimensional spatial modelling of on-nuclear spectra to obtain generally young host ages ($\lesssim$2 Gyr). Thus, the few studies which to date combine broad-band and spectral information are internally consistent but give differing results.

This could possibly be caused by a difference in host population since the Nolan et al. objects are brighter and larger than those of Jahnke, but the different relative positions in the host galaxy where the spectra were registered may also be of importance. While the spectra of Jahnke are on-nuclear, the spectra

of Nolan et al. were taken at a distance of ∼5″ from the nucleus. In the quasar composite spectra of Vanden Berk et al. (2001), which were obtained within a 3″ diameter optical fibre, stellar Balmer absorption lines are seen in both low and high redshift composites, implying that young or intermediate age stars make a substantial contribution to the host galaxy light. Note also the contradictory fits of Nolan et al. and Canalizo & Stockton (2000) for the object Mrk 1014 (an infrared-loud RQQ at $z = 0.1634$). The former find a contribution of young stars of 1%, while the latter discover several recent star formation regions and obtain a value of 8−12% by mass for the young stellar light contribution. Taken together, this is suggestive of a younger stellar population closer to the nuclei of the hosts, much as expected in merger scenarios for nuclear activity.

The spectral fitting by Jahnke (2002) does not indicate strong starbursts taking place in the investigated host galaxies, which however are found to be gas rich. This is in accordance with the results of Scoville et al. (2003), who detect H_2 molecular gas masses in excess of 10^9 $M_\odot$ in a majority of quasar host galaxies at low redshifts ($\lesssim$0.1). The gas masses of normal elliptical galaxies amount to $\lesssim 10^8$ $M_\odot$ while late-type galaxies mostly have $M_{H_2} \gtrsim 10^9$ $M_\odot$ (Georgakakis et al. 2001; Casoli et al. 1998, and references therein), making the host galaxies atypically gas rich for being ellipticals.

In sum, spectroscopical investigations of host galaxies at low redshift possibly indicate two different kinds of population (Jahnke 2002), which also could be separated by their broadband colours. Extending such colour studies to encompass a larger range of filters promises the possibility of evaluating the stellar populations of host galaxies even at higher redshifts. In the light of the growing evidence for blue host colours at low as well as intermediate redshifts, such studies can help distinguish the processes responsible for these colours and, by comparison to both the normal galaxy population and the blue non-active elliptical galaxies, provide clues to the triggering and fuelling of nuclear activity.

5. Conclusions

We have carried out a large optical imaging study of quasar host galaxies at $0.4 \leq z \leq 0.8$, which constitutes roughly half the number of the investigated sources in the intermediate redshift regime and specifically extends the number of resolved radio-quiet hosts at $z > 0.4$ by a substantial amount. Out of 91 analysed fields obtained at the NTT and the NOT telescopes, hosts were detected in a total of 66 sources or 72% of the samples where the detection rate of radio-loud sources is 79%, while that of the radio-quiet hosts is 66%. The detection rate was, however, much lower in the sample of objects placed at our disposal by Wold et al. (2000, 2001).

We find that the axial ratios of both radio-loud and radio-quiet hosts peak at $b/a \gtrsim 0.8$ in the same manner as for the normal elliptical galaxy population. For the majority of the sample, profile fitting could not be carried out, but for the subsample where a morphology could be determined, the objects are found to be predominantly of elliptical type.

The mean absolute magnitude of the radio-quiet hosts is $M_R = -23.5 \pm 0.2$, which is indistinguishable from that of the radio-loud hosts. A similar result is found in the V band, but a slightly larger difference can be seen in the I band where the mean of the radio-quiet hosts is $M_I = -23.4 \pm 0.2$ and that of the radio-loud hosts $M_I = -23.8 \pm 0.2$. This deviates from the results at lower redshifts where a mean difference of ∼0.5 mag is found between radio-loud and radio-quiet hosts. The magnitudes of the radio-loud hosts brighten over the redshift range investigated, connecting to low redshift hosts from the literature and extending towards the bright radio-loud sources found in studies at higher redshift. The radio-quiet hosts remain of a more similar brightness over the range, with only a weak dependence on redshift. However, note that the detection limit of the NON sample in combination with the relationship between host and nuclear luminosity may create a spurious brightening effect with redshift, in that larger volumes are sampled, while faint hosts become increasingly difficult to resolve and thus fall out of the sample.

Examination of the nucleus-to-host luminosity ratios reveal no differences between resolved radio-loud and radio-quiet sources in any of the imaged bands. Comparison of the ratios for FS and SS radio sources shows that the mean luminosity ratio of the FS objects differs from that of the SS objects only at the 1.5σ level, in contrast to previous results (Kotilainen & Falomo 2000). The mean luminosity ratios for these two subclasses, as computed for the low redshift radio-loud sources of Hamilton et al. (2002), also do not differ significantly. Investigation of the host-nucleus luminosity limit results in an upper bound consistent with objects which radiate at an Eddington ratio of ∼5% for both radio-loud and radio-quiet sources (but see also the discussion in Sect. 4.2.3).

The host galaxy colours are found to be as blue as those of present-day late-type disks and starburst objects, with no difference between the mean $V - R$ colour of radio-quiet and radio-loud hosts. To investigate the impact of scattered nuclear light as a contributor to the host colours, we also measured the colours in annular apertures. The difference between full and annular aperture values is in general <0.1 mag, implying a negligible contribution of scattered light. The effect of galaxy evolution over the redshift range only influences the colours by $\lesssim$0.2 mag and is thus also not a major contributor to the blue host colours.

The mean difference in $V - R$ between the hosts and template normal elliptical galaxies at the same redshifts is ∼0.7 mag, while the mean difference in $R-I$ is ∼0.6 mag. There is no morphological indication that the hosts are of late Hubble type, and close companions in projection are not uncommon, with a few sources even exhibiting tidal tail-like features and other signs of interaction. Thus, ongoing star formation is a reasonable explanation of the blue host colours. As the multiband imaging was primarily performed for such objects where the presence of a host galaxy was indicated, the colour analysis cannot safely be generalised to hold for the quasar host galaxy population at intermediate redshifts as a whole. Note, however, that the blue trend of the colours derived in this paper are in good agreement with the few previous colour studies of host galaxies at these redshifts (Kirhakos et al. 1999; Sánchez et al. 2004).

At low redshift, recent work in broad-band colours, as well as in spectroscopy, indicates the possible existence of two different populations of host galaxies: one blue and gas rich, the other larger and redder (Jahnke 2002; Dunlop et al. 2003). In order to properly address the connection between lower redshift hosts and those found at intermediate redshifts, further observations are needed. Knowledge of the proper morphological types of the hosts will permit application of appropriate K-corrections and also enable the scale lengths to be determined. By using broad-band colours over large wavelength baselines, the circumstances giving rise to the blue host colours can be better defined. The new on-nuclear spectroscopical techniques (Jahnke 2002; Courbin et al. 2002) also promise the possibility of studying the stellar populations of the host galaxies at lower redshifts in greater detail, whereas further targetting of hosts at redshifts $\sim 0.7-1$ will provide information on host galaxy evolution. Of particular interest is the comparison of quasar hosts to non-active galaxies, especially to the population of blue early-type galaxies that have been identified recently (e.g. Cross et al. 2004; Sánchez et al. 2004). A dedicated effort to increase the number of investigated radio-quiet sources at redshifts above ~ 0.5 is also needed.

Acknowledgements. Dr. Margrethe Wold and collaborators are cordially thanked for granting us access to the Wold data. We also wish to thank the anonymous referee for her perceptive comments which helped improve aspects of this paper. This research made use of the following resources: NASA/IPAC Extragalactic Database (NED), which is operated by the Jet Propulsion Laboratory, California Institute of Technology, under contract with the National Aeronautics and Space Administration; NASA's Astrophysics Data System Abstract Service; the SIMBAD database, operated at CDS, Strasbourg, France.

References

Abraham, R. G., Ellis, R. S., Fabian, A. C., Tanvir, N. R., & Glazebrook, K. 1999, MNRAS, 303, 641
Aretxaga, I., Le Mignant, D., Melnick, J., Terlevich, R. J., & Boyle, B. J. 1998, MNRAS, 298, L13
Bahcall, J. N., Kirhakos, S., Saxe, D. H., & Schneider, D. P. 1997, ApJ, 479, 642
Becker, R., White, R. L., & Helfand, D. J. 1995, ApJ, 450, 559
Bell, E. F., McIntosh, D. H., Barden, M., et al. 2004, ApJ, 600, L11
Block, D. L., & Stockton, A. 1991, AJ, 102, 1928
Boyce, P. J., Disney, M. J., Blades, J. C., et al. 1996, ApJ, 473, 760
Boyce, P. J., Disney, M. J., Blades, J. C., et al. 1998, MNRAS, 298, 121
Brotherton, M. S., Grabelsky, M., Canalizo, G., et al. 2002, PASP, 114, 593
Bruzual, G., & Charlot, S. 2003, MNRAS, 344, 1000
Calzetti, D., Kinney, A. L., & Storchi-Bergmann, T. 1994, ApJ, 429, 582
Canalizo, G., & Stockton, A. 2000, AJ, 120, 1750
Canalizo, G., & Stockton, A. 2001, ApJ, 555, 719
Carballo, R., Sánchez, S. F., González-Serrano, J. I., Benn, C. R., & Vigotti, M. 1998, AJ, 115, 1234
Casoli, F., Sauty, S., Gerin, M., et al. 1998, A&A, 331, 451
Cimatti, A., Dey, A., van Breugel, W., Antonucci, R., & Spinrad, H. 1996, ApJ, 465, 145
Courbin, F., Letawe, G., Magain, P., et al. 2002, A&A, 394, 863
Cross, N. J. G., Bouwens, R. J., Benítez, N., et al. 2004, AJ, 128, 1990
de Vries, W. H., O'Dea, C. P., Baum, S. A., et al. 1997, ApJS, 110, 191
Dey, A., Cimatti, A., van Breugel, W., Antonucci, R., & Spinrad, H. 1996, ApJ, 465, 157
Dunlop, J. S., McLure, R. J., Kukula, M. J., et al. 2003, MNRAS, 340, 1095
Ellingson, E., & Yee, H. K. C. 1994, ApJS, 92, 33
Falomo, R., Urry, C. M., Pesce, J. E., et al. 1997, ApJ, 476, 113
Falomo, R., Kotilainen, J., & Treves, A. 2001, ApJ, 547, 124
Ferrarese, L., Pogge, R. W., Peterson, B. M., et al. 2001, ApJ, 555, L79
Fioc, M., & Rocca-Volmerange, B. 1997, A&A, 326, 950
Fosbury, R. 1997, in Quasar Hosts, ed. Clements & Pérez-Fournon, ESO Conf. Ser., 3
Fukugita, M., Shimasaku, K., & Ichikawa, T. 1995, PASP, 107, 945
Gehren, T., Fried, J., Wehinger, P. A., & Wyckoff, S. 1984, ApJ, 278, 11
Georgakakis, A., Hopkins, A. M., Caulton, A., et al. 2001, MNRAS, 326, 1431
Hamilton, T. S., Casertano, S., & Turnshek, D. A. 2002, ApJ, 576, 61
Hewett, P. C., Foltz, C. B., & Chaffee, F. H. 1995, AJ, 109, 1498
Hewitt, A., & Burbidge, G. 1993, ApJS, 87, 451
Hooper, E., Impey, C., & Foltz, C. 1997, ApJ, 480, 95
Hughes, D. H., Kukula, M. J., Dunlop, J. S., & Boroson, T. 2000, MNRAS, 316, 204
Hutchings, J. B., & Morris, S. C. 1995, AJ, 109, 1541
Hutchings, J. B., & Neff, S. G. 1990, AJ, 99, 1715
Hutchings, J. B., & Neff, S. G. 1992, AJ, 104, 1
Hutchings, J. B., Frenette, D., Hanisch, R., et al. 2002, AJ, 123, 2936
Im, M., Faber, S. M., Gebhardt, K., et al. 2001, AJ, 122, 750
Ivezić, Z., Menou, K., Knapp, G. R., et al. 2002, AJ, 124, 2364
Jahnke, K. 2002, Ph.D. Thesis, Universität Hamburg
Jahnke, K., Kuhlbrodt, B., & Wisotzki, L. 2004, MNRAS, 352, 399
Keel, W. C. 1980, AJ, 85, 198
Kellermann, K. I., Sramek, R., Schmidt, M., Shaffer, D. B., & Green, R. 1989, AJ, 98, 1195
Kinney, A. L., Calzetti, D., Bohlin, R. C., et al. 1996, ApJ, 467, 38
Kirhakos, S., Bahcall, J. N., Schneider, D. P., & Kristian, J. 1999, ApJ, 520, 67
Kotilainen, J. K., & Falomo, R. 2000, A&A, 364, 70
Kotilainen, J. K., Falomo, R., & Scarpa, R. 1998, A&A, 332, 503
Krempeć-Krygier, J., Krygier, B., & Walentynowicz, G. 1998, A&A, 334, 427
Kukula, M. J., Dunlop, J. S., McLure, R. J., et al. 2001, MNRAS, 326, 1533
Lambas, D. G., Maddox, S. J., & Loveday, J. 1992, MNRAS, 258, 404
Laor, A. 1998, ApJ, 505, L83
Lin, H., Kirshner, R. P., Shectman, S. A., et al. 1996, ApJ, 464, 60
MacKenty, J. W. 1990, ApJS, 72, 231
Magorrian, J., Tremaine, S., Richstone, D., et al. 1998, AJ, 115, 2285
Márquez, I., Durret, F., & Petitjean, P. 1999, A&AS, 135, 83
Márquez, I., Petitjean, P., Théodore, B., et al. 2001, A&A, 371, 97
McLeod, K. K., & McLeod, B. A. 2001, ApJ, 546, 782
McLeod, K. K., & Rieke, G. H. 1994, ApJ, 420, 58
McLeod, K. K., & Rieke, G. H. 1995, ApJ, 441, 96
McLeod, K. K., Rieke, G. H., & Storrie-Lombardi, L. J. 1999, ApJ, 511, L67
McLure, R. J., & Dunlop, J. S. 2002, MNRAS, 331, 795
Menanteau, F., Ellis, R. S., Abraham, R. G., Barger, A. J., & Cowie, L. L. 1999, MNRAS, 309, 208
Menanteau, F., Ford, H. C., Illingworth, G. D., et al. 2004, ApJ, 612, 202

Merritt, D., & Ferrarese, L. 2001, ApJ, 547, 140
Natali, F., Giallongo, E., Cristiani, S., & La Franca, F. 1998, AJ, 115, 397
Nolan, L. A., Dunlop, J. S., Kukula, M. J., et al. 2001, MNRAS, 323, 308
O'Dea, C. P., de Vries, W., Biretta, J. A., & Baum, S. A. 1999, AJ, 117, 1143
Örndahl, E., Rönnback, J., & van Groningen, E. 2003, A&A, 404, 883 (Paper I)
Percival, W. J., Miller, L., McLure, R. M., & Dunlop, J. S. 2001, MNRAS, 322, 843
Poggianti, B. M. 1997, A&AS, 122, 399
Pursimo, T., Nilsson, K., Takalo, L. O., et al. 2002, A&A, 381, 810
Ridgway, S. E., Heckman, T. M., Calzetti, D., & Lehnert, M. 2001, ApJ, 550, 122
Romanishin, W., & Hintzen, P. 1989, ApJ, 341, 41
Rönnback, J., & Bergvall, N. 1994, A&AS, 108, 193
Rönnback, J., van Groningen, E., Wanders, I., & Örndahl, E. 1996, MNRAS, 283, 282 (R96)
Saglia, R. P., Bertschinger, E., Baggley, G., et al. 1993, MNRAS, 264, 961
Sánchez, S. F., Jahnke, K., Wisotzki, L., et al. 2004, ApJ, 614, 586
Sandage, A., Freeman, K. C., & Stokes, N. R. 1970, ApJ, 160, 831
Scarpa, R., Urry, C. M., Falomo, R., Pesce, J. E., & Treves, A. 2000, ApJ, 532, 740
Schade, D., Lilly, S. J., Crampton, D., et al. 1999, ApJ, 451, L1
Schade, D. J., Boyle, B. J., & Letawsky, M. 2000, MNRAS, 315, 498
Schlegel, D. J., Finkbeiner, D. P., & Davis, M. 1998, ApJ, 500, 525
Scoville, N. Z., Frayer, D. T., Schinnerer, E., & Christopher, M. 2003, ApJ, 585, L105
Stockton, A. 1990, in Dynamics and Interactions of Galaxies, ed. R. Wielen (Springer), 440
Stockton, A., & MacKenty, J. W. 1987, ApJ, 316, 584
Stockton, A., MacKenty, J. W., Hu, E. M., & Kim, T. 2002, ApJ, 572, 735
Tadhunter, C., Dickson, R., Morganti, R., et al. 2002, MNRAS, 330, 977
Urry, C. M., & Padovani, P. 1995, PASP, 107, 803
Urry, C. M., Falomo, R., Scarpa, R., et al. 1999, ApJ, 512, 88
Vanden Berk, D. E., Richards, G. T., Bauer, A., et al. 2001, AJ, 122, 549
Városi, F., & Dwek, E. 1999, ApJ, 523, 265
Véron-Cetty, M. P., & Véron, P. 1993, ESO Sci. Rep., 13
Véron-Cetty, M.-P., & Woltjer, L. 1990, A&A, 236, 69
Wandel, A. 2002, ApJ, 565, 762
White, R. L., Becker, R. H., Gregg, M. D., et al. 2000, ApJS, 126, 133
Witt, A. N., & Gordon, K. D. 1996, ApJ, 463, 681
Witt, A. N., & Gordon, K. D. 2000, ApJ, 528, 799
Wold, M., Lacy, M., Lilje, P. B., & Serjeant, S. 2000, MNRAS, 316, 267
Wold, M., Lacy, M., Lilje, P. B., & Serjeant, S. 2001, MNRAS, 323, 231
York, D. G., Adelman, J., Anderson, J. E., J., et al. 2000, AJ, 120, 1579

Online Material

Appendix A: Wold quasar host images and profiles

In Fig. A.1 we show images and luminosity profiles of the Wold sample quasars and host galaxies, presented in order of right ascension. All fields shown were observed in *R* band. The non-calibrated object 7C 2671 is indicated by a #-symbol.

For each object field and filter, we present five plots. In the leftmost graph the luminosity profile is plotted (in mag arcsec^{-2}) versus radius in arcseconds. The points represent the quasar profile, the full-drawn line is the PSF, and the dotted line the residual after PSF subtraction. In the fourfold greyscale plot the image sizes are always $12\farcs5 \times 12\farcs5$, with the objects centred in the plots. Top left shows the host galaxy residual, top right is the unsubtracted quasar frame, and in the bottom right graph we show the residual left from the scaling of the PSF to a field star. The bottom left graph is a contour plot of the host galaxy residual, where the number inside the plot denotes the value of the lowest contour in mag arcsec^{-2} and the spacing between contours is 1 mag arcsec^{-2}. The contours have been smoothed by a 3×3 box for better clarity of low-intensity features. North is up and east is to the left.

Appendix B: Notes on selected individual objects

In this Appendix we present notes on selected NOT and Wold objects only. A discussion of the properties of individual NTT sources can be found in R96. All quoted absolute magnitudes and distances have been transformed to the cosmology used in this paper ($H_0 = 75$ km s^{-1} Mpc^{-1} and $q_0 = 0.5$) for ease of comparison.

B.1. MRC 0032–203

This radio-loud source at $z = 0.518$ seems to be connected by a bridge to a galaxy at a projected distance of 37 kpc. The magnitude of this galaxy is $R = 21.1$.

B.2. 3C 138

This object at $z = 0.759$ was observed and marginally resolved by Kotilainen & Falomo (2000) in *H* band, resulting in a magnitude of the nucleus of $M_H = -24.9$ and a host magnitude of $M_H = -24.2$. Imaging by Hutchings & Neff (1990) in *R* band yields a nuclear magnitude of $M_R = -23.9$ and a host magnitude of $M_R = -24.0$. This is similar to the values found in this paper of $M_R = -24.4$ for the nucleus and $M_R = -24.1$ for the host.

B.3. GC 0742+3321

The flat-spectrum source GC 0742+3321 at $z = 0.610$ and MC 2142+1101 (also a flat-spectrum source, located at $z = 0.55$) are those two objects which are redder than an Sb galaxy and which have a <0.1 mag difference between the full and the annular colour (see Sect. 4.3). The host of MC 2142+1101 is large and smooth, but the host of GC 0742+3321 displays a very elongated structure. This structure was not included in the magnitude measurements, since it also could be a very close companion or perhaps an extended emission line envelope. An envelope would mainly contribute in the *I* band at this *z*, and since the colour of the elongated part is $R - I = 0.7$, it is more likely that the structure is either a very closely placed companion galaxy or perhaps a starforming region in the host galaxy itself.

B.4. 3C 275.1

This well-known source at $z = 0.555$ has been studied in many aspects. It is at the centre of the galaxy group it is associated with (Krempeć-Krygier et al. 1998). The close companion to the south-east is at the same redshift as the quasar (Ellingson & Yee 1994) and thus separated from the host by 28 kpc, but the object in close projection to the north-west is a foreground object. The magnitude of the companion is $R = 21.0$, in good agreement with the value obtained by Ellingson & Yee of $R = 21.22$.

Márquez et al. (1999) have performed imaging in *J* band and derive a host magnitude of $M_J = -24.8$. Combined with our *R* magnitude, this leads to the quite blue $R - J$ colour of 0.9. In comparison, an elliptical galaxy at this redshift has a colour of $R - J = 1.5$ while an Sc spiral galaxy has $R - J = 1.1$ (Fioc & Rocca-Volmerange 1997).

B.5. B2 1512+3701

This object at $z = 0.37$ has a well-known extended emission line region in [OIII]λ5007, which is the most luminous known among quasars at $z \lesssim 0.5$ (Stockton & MacKenty 1987; Block & Stockton 1991). Imaging with the HST in [OIII] reveals extraordinary detail and indicates that this structure is ionised by the quasar (Stockton et al. 2002).

The quasar has also been observed by Hamilton et al. (2002) with the HST. Two-dimensional fitting of the host image performed by these authors results in a nuclear magnitude of $M_V = -24.5$ and a host magnitude of $M_V = -22.8$. In good agreement, we derive $M_V = -24.1$ for the nucleus and $M_V = -22.9$ for the host.

B.6. PG 1543+4855

We resolved this host galaxy at $z = 0.40$ in *R* and *V* band, and marginally in the *I* band. In all bands a faint connection can be seen between the host and a compact object only 25 kpc to the south. The magnitude of this companion is $R = 20.2$. Imaging by Canalizo & Stockton (2001) reveals a bridge in *V* between the two objects, but only a knot in K'. From spectral information the companion is shown to be a galaxy at $z = 0.4$ which has experienced a starburst ~200 Myr ago. The host spectrum is similar to that of the companion although noisier, but the host appears to be slightly bluer. Faint [OII] and [OIII] emission is visible in a small clump along the connecting bridge. These aspects all indicate strong interaction between the host and the companion.

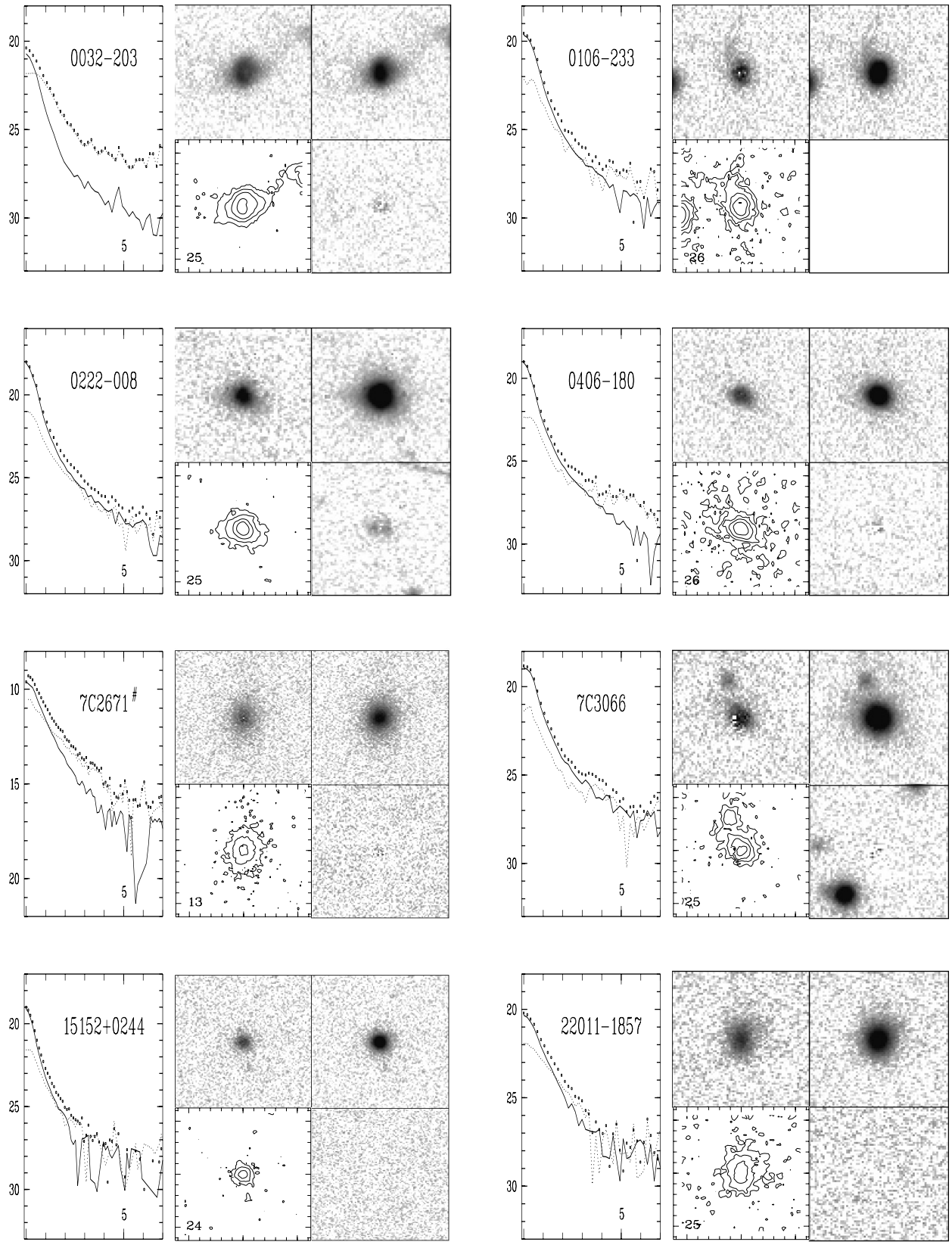

Fig. A.1. Images and profiles of the Wold quasars and host galaxies. For each object field and filter we present the luminosity profile in mag arcsec^{-2} with radius in arcsec (points: quasar profile; full-drawn line: PSF; dotted line: residual); centred greyscale images of residual (*top left*), unsubtracted quasar (*top right*) and test star remainder (*bottom right*); contour plot of the residual (number inside the frame is the lowest contour level in mag arcsec^{-2}; spacing of contours is 1 mag arcsec^{-2}). The image sizes are 12.″5 to a side. North is up and east is to the left.

Percival et al. (2001) have observed this object and derive a disk-like profile with an axial ratio of 0.89, while we find $b/a = 0.84$. The host galaxy K band magnitude is $M_K = -24.4$, which combined with our R value results in a colour of $R-K = 0.7$, bluer even than what would be expected 200 Myr after a starburst. The $V - R$ annular colour derived in this paper is, however, consistent with this age (Fioc & Rocca-Volmerange 1997).

B.7. MC 1548+1129

This host located at $z = 0.436$ was also observed by Hamilton et al. (2002) with the HST. Their two-dimensional fit determines the morphology to be that of a spiral host, despite the fact that this quasar is radio-loud. The possible large tidal arm seen by Hamilton et al. may, however, be responsible for the better fit of the exponential disk. No images are presented in their paper, but in our own image at much lower resolution, a faint feature to the east is present. Hamilton et al. find a nuclear V magnitude of $M_V = -22.78$ and a host magnitude of $M_V = -21.32$. Combining their V band with our R band data results in $V - R = 0.48$, similar to that of an Sc or starburst galaxy. The immediate surroundings of this object are also of interest: at a projected distance of 65 kpc three galaxies form a very tight group with a maximum distance between the members of only ∼13 kpc (assuming their redshift to be that of the quasar).

B.8. 4C 40.37

For this object with a redshift of $z = 0.733$, Hutchings & Neff (1990) derive a nuclear magnitude of $M_R = -24.0$ and a host magnitude of $M_R = -24.6$. This is in good agreement with the values found in this paper of $M_R = -24.0$ for the nucleus and $M_R = -24.3$ for the host.

B.9. 4C 56.27

This object at $z = 0.664$ is a BL Lac source. It was observed with the Nordic Optical Telescope by Pursimo et al. (2002) during very similar seeing conditions and with a similar exposure time to ours, resulting in an apparent total magnitude of $R = 18.1$ as compared to our value of $R = 18.23$. With a de Vaucouleur-fitted profile the host magnitude obtained by Pursimo et al. is $R = 19.75$, while a disk fit yields $R = 20.51$, which compares well to our value of $R = 20.5$. The luminosity profiles also agree quite well.

The object was observed with HST and R band magnitudes obtained by Scarpa et al. (2000), who find a total magnitude of $R = 18.02$, while the host magnitude is determined to be $R = 20.24$ for a de Vaucouleurs law fit and $R = 21.14$ for a disk fit. Urry et al. (1999) determine the total I band magnitude to be $I = 17.4$, while a de Vaucouleurs law fit yields $I = 18.80$ for the host galaxy and a disk fit results in $I = 19.63$ mag. In comparison, the I band values derived by us are for the quasar $I = 17.52$ mag and for the host $I = 19.1$ mag, again in good agreement.

Urry et al. compute a colour profile in $V - I$ and find no large gradient over the investigated radius range ($0\farcs5$–$2\farcs5$). The mean $V - I$ value is ∼2.8, consistent with the colour of a normal elliptical galaxy at this redshift. The $R - I$ colour determined from the literature values is $R - I = 1.44$ (de Vaucouleur fit) respectively $R - I = 1.51$ (disk fit), while the colour obtained by us is $R - I = 1.4$. This is consistent with the $R - I$ colour of an elliptical galaxy at this redshift of $R - I = 1.44$ from Fukugita et al. (1995).

Falomo et al. (1997) discuss the immediate surroundings and the non-stellar object located at a projected distance of 24 kpc to the east of the source. For this object we obtain a magnitude of $R = 21.6$. The distortion of this possible companion, which shows asymmetric emission elongated towards the south, could indicate tidal interaction with the host galaxy. Falomo et al. also compare the HST luminosity profile to ground-based R band imaging obtained at the NOT and find excellent agreement.

B.10. 3C 380

No host is detected in R band for this object at $z = 0.692$, though it is clearly present in V and I band. However, there is an off-centred structure visible in all bands, which coincides with the two optical synchrotron hotspots detected by de Vries et al. (1997) with HST. There is very little [OII]λ3727 line emission in the aligned component, suggesting that the optical continuum light dominates the two knots (O'Dea et al. 1999).

B.11. 2217+0845

This slightly off-centred host at $z = 0.623$ is situated in a rich field and has also been observed by Romanishin & Hintzen (1989) in B band. The derived quasar M_B magnitude is −23.3, while the host has $M_B = -21.6$ mag. Combining this value with the R band magnitude derived by us results in $B-R = 1.7$, similar to the colour of an Sc galaxy. The $R - I$ colour found in Sect. 4.3 indicates colours as blue as those of a starburst galaxy. The luminosity ratio derived by Romanishin & Hintzen is 7.1, which is higher than the values found in this paper for R and I band, consistent with the decreasing significance of host galaxy light at shorter wavelengths.

B.12. PKS 2351–0036

This object at $z = 0.46$ is resolved in our data, but was observed during non-photometric conditions. It is included in the study by Hooper et al. (1997), who derive a total quasar R magnitude of $M_R = -23.3$. With a disk fit, the host magnitude is determined to $M_R = -20.82$ mag, while a de Vaucouleurs profile results in $M_R = -22.14$ mag. The luminosity ratio is 14.1 for the disk fit and 6.2 for the elliptical fit, which is closer to the value of 4.1 derived in this paper. Hooper et al. find an axial ratio of 0.4, while we find $b/a = 0.9$. The images presented for this object in Paper I and in Hooper et al. both show a centrally concentrated host, though the Hooper et al. image has a slight extension towards the SE not present in the NOT image.